

BAYESIAN DETECTION OF IMAGE BOUNDARIES

BY MENG LI* AND SUBHASHIS GHOSAL*

Duke University and North Carolina State University

Detecting boundary of an image based on noisy observations is a fundamental problem of image processing and image segmentation. For a d -dimensional image ($d = 2, 3, \dots$), the boundary can often be described by a closed smooth $(d - 1)$ -dimensional manifold. In this paper, we propose a nonparametric Bayesian approach based on priors indexed by \mathbb{S}^{d-1} , the unit sphere in \mathbb{R}^d . We derive optimal posterior contraction rates using Gaussian processes or finite random series priors using basis functions such as trigonometric polynomials for 2-dimensional images and spherical harmonics for 3-dimensional images. For 2-dimensional images, we show a rescaled squared exponential Gaussian process on \mathbb{S}^1 achieves four goals of guaranteed geometric restriction, (nearly) minimax optimal rate adaptive to the smoothness level, convenient for joint inference and computational efficiency. We conduct an extensive study of its reproducing kernel Hilbert space, which may be of interest by its own and can also be used in other contexts. Several new estimates on the modified Bessel functions of the first kind are given. Simulations confirm excellent performance of the proposed method and indicate its robustness under model misspecification at least under the simulation settings.

1. Introduction. The problem of detecting boundaries of image arise in a variety of areas including epidemiology [44], geology [26], ecology [12], forestry, marine science. A general d -dimensional ($d \geq 2$) image can be described as $(X_i, Y_i)_{i=1}^n$, where $X_i \in T = [0, 1]^d$ is the location of the i th observation and Y_i is the corresponding pixel intensity. Let $f(\cdot; \phi)$ be a given regular parametric family of densities, with respect to a σ -finite measure ν , indexed by a p -dimensional parameter $\phi \in \Theta$, then we assume that there is a closed region $\Gamma \subset T$ such that

$$Y_i \sim \begin{cases} f(\cdot; \xi) & \text{if } X_i \in \Gamma; \\ f(\cdot; \rho) & \text{if } X_i \in \Gamma^c, \end{cases}$$

where ξ, ρ are distinct but unknown parameters. We assume that both Γ and Γ^c have nonzero Lebesgue measures. The goal here is to recover the boundary

*Research partially supported by NSF grant number DMS-1106570.

MSC 2010 subject classifications: Primary 62G20, 62H35; secondary 62F15, 60G15

Keywords and phrases: Boundary detection, Gaussian process on sphere, image, posterior contraction rate, random series, squared exponential periodic kernel, Bayesian adaptation

$\gamma = \partial\Gamma$ from the noisy image where γ is assumed to be a smooth $(d - 1)$ -dimensional manifold without boundary, and derive the contraction rate of γ at a given true value γ_0 in terms of the metric defined by the Lebesgue measure of the symmetric difference between the regions enclosed by γ and γ_0 . When the boundary itself is of interest such as in image segmentation, we can view the problem as a generalization of the change-point problem in one dimensional data to images.

A significant part of the literature focuses on the detection of boundary pixels, based on either first-order or second-order derivatives of the underlying intensity function [32, Ch. 6] or Markov random fields [13, 14], resulting in various edge detectors or filters. This approach is especially popular in computer vision [3, 4]. However, the detected boundary pixels are scattered all over the image and do not necessarily lead to a closed region, and hence cannot be directly used for image segmentation. A post-smoothing step can be applied, such as Fourier basis expansion, principal curves [18] or a Bayesian multiscale method proposed by [16]. However the ad-hoc two-step approach makes the theoretical study of convergence intractable. In addition, as pointed out by [2], many applications produce data at irregular spatial locations and do not have natural neighborhoods.

Most existing methods are based on local smoothing techniques [5, 38, 17, 31, 34], which lead to convenient study of theoretical properties benefiting from well established results. However, local methods suffer when the data is sparse and thus the usage of the global information becomes critical. More importantly, it often leads to *local* (or pointwise) inference such as marginal confidence bands losing the joint information.

A relevant and intensively studied problem is to estimate the underlying intensity function $E(Y|X)$ with discontinuity at the boundary [29, 36, 9, 17, 33, 35]. These two problems are different for at least two reasons. First, there are many important applications where ξ and ρ affect $f(\cdot)$ not (or not only) in the mean but some other characteristics such as variance [5]. Second, the reconstruction of $E(Y|X)$ is essentially a curve (or surface) fitting problem with discontinuity and the corresponding asymptotics are mostly on the entire intensity function rather than the boundary itself. Therefore, we may refer the latter as image denoising when boundaries are present, not necessarily guaranteeing the geometric restrictions on the boundary such as closedness and smoothness.

In this paper, we propose a nonparametric Bayesian method tailored to detect the boundary γ_0 , which is viewed as a closed smooth $(d - 1)$ -dimensional manifold without boundary. This paper has three main contributions.

The first main contribution is that the proposed method is, to our best knowledge, the first one in the literature that achieves all the following four goals (i)–(iv) when estimating the boundary.

- (i). Guaranteed geometric restrictions on the boundary such as closedness and smoothness.
- (ii). Convergence at the (nearly) minimax rate [23, 28], adaptively to the smoothness of the boundary.
- (iii). Possibility and convenience of joint inference.
- (iv). Computationally efficient algorithm.

To address (i) and (iii), the Bayesian framework has its inherent advantages. For (i), we note that Bayesian methods allow us to put the restrictions on the boundary conveniently via a prior distribution. Specifically, we propose to use a Gaussian process (GP) prior indexed by the unite sphere in \mathbb{R}^d , i.e. the $(d-1)$ -sphere $\mathbb{S}^{d-1} = \{x = (x_1, \dots, x_d) \in \mathbb{R}^d : x_1^2 + \dots + x_d^2 = 1\}$, and a random series prior on \mathbb{S}^{d-1} . For (iii), Bayesian methods allow for joint inference since we draw samples from the joint posterior distributions, as demonstrated by the numerical results in Section 6. The proposed method achieves the (nearly) minimax optimal rate adaptive to the unknown smoothness level based on a random rescaling incorporated by a hierarchical prior [43, 39]. Furthermore, Goal (ii) is achieved for any regular family of noise and general dimensions. In contrast, for instance, the method in [28] is only for two-dimensional binary images and does not adapt to the unknown smoothness level. Although the qualification of uncertainty and adaptivity of a method is appealing, the computation in goal (iv) is important when implementing it. Many adaptive methods are hard to implement since inverses of covariance matrices need to be calculated repeatedly. In the proposed Bayesian approach, an efficient Markov chain Monte Carlo (MCMC) sampling is designed based on the analytical eigen decomposition of the squared exponential periodic (SEP) kernel (see Section 5), for various noise distributions. In addition, we conduct extensive numerical studies to confirm the good performance of the proposed method and indicate that it is robust under model misspecification at least under the simulated settings.

As the second main contribution, we conduct an extensive study on the reproducing kernel Hilbert space (RKHS) of the SEP Gaussian process, which is essential to obtain the optimal rate and adaptation in Goal (ii). For the most important case in applications $d = 2$, by a simple mapping, the squared exponential (SE) Gaussian process on \mathbb{S}^1 is equivalent to a SEP Gaussian process on $[0, 1]$ since their RKHS's are isometric (see Lemma 3.2). Recently developed theory of posterior contraction rates implies that nonparametric

Bayesian procedures can automatically adapt to the unknown smoothness level using a rescaling factor via a hyperparameter in a stationary Gaussian processes on $[0, 1]$ or $[0, 1]^d$ [41, 43]. Rescaled SE Gaussian process is one popular example of this kind. In contrast, the literature lacks results on the rescaling scheme and the resulting properties of the SEP Gaussian process, even though it has been implemented in many applications [27]. It may be due to the seemingly similarity shared between the SEP Gaussian process and the SE Gaussian process. However, we figure out that these two processes have fundamental differences. This is because that the rescaling of the argument on \mathbb{S}^1 cannot be transformed as a rescaling of the mapped argument on the Euclidean domain. Instead, the rescaling factor rescales a kernel function not directly on the argument but outside the sine function in the exponential. In addition, the spectral measure of the SEP Gaussian process is discrete (see Lemma 4.1) thus lacking the absolute continuity of that of the SE Gaussian process which is critical in establishing many of its properties [43]. As a result, the RKHS of the SEP Gaussian process for different scales do not follow some of the properties of that of the SE Gaussian process, for example, the usual nesting property. We overcome these issues by using the special eigen structure of the SEP kernel and intriguing properties of the modified Bessel functions of the first kind. Some of the properties of the SE Gaussian process still hold, however, the proofs are remarkably different. Nevertheless, we show that the posterior contraction rate of the boundary by using the SEP Gaussian process is nearly minimax-optimal, which is $n^{-\alpha/(\alpha+1)}$ up to a logarithmic factor, adaptively to the smoothness level α of the boundary. Section 4 establishes a list of properties on the RKHS of the SEP Gaussian process, along with the contraction rate calculation and adaptation.

The third main contribution is that we provide some new estimates on Bessel functions, which are critical when establishing properties on the RKHS of the SEP Gaussian process. Similar to the second main contribution, these new estimates may be of interest by their own and are useful in broader contexts such as function estimation on spheres in addition to the boundary detection problem discussed here.

In addition to establishing key theoretical properties, we also develop a very efficient MCMC method for sampling posterior distribution based on a SEP Gaussian process prior using the explicit eigen structure of the SEP Gaussian process obtained in this paper. The algorithm is generic and hence can be used for posterior computation in other curve estimation problems on the circle such as directional data analysis while using the SEP Gaussian process prior.

The proposed method with theoretical supports and numerical confirmation is intriguing in the sense that it could be applied, with or without modifications, to many applications. Depending on the concrete context, an image may have multiple objects or objects with boundaries that are not star-shaped. If only one object is of interest in a multiple-object image, such as the case in brain imaging where we want to detect a tumor boundary, the proposed method can be applied by using a mixture distribution as the noise distribution f . If multiple objects are of interest, some adjustment may be needed, for example, in a “divide-and-conquer” fashion by applying the method multiple times for each objects. For non star-shaped objects, the implementation of the proposed method may lead to a star-shaped approximation to the targeted boundary. There are many other interesting directions that the current paper leads to, such as when the boundary has heterogeneous smoothness (for example, the smoothness parameter α varies spatially) and to address unknown number of objects. By providing a Bayesian framework to boundary detection problem whose good performance and robustness to misspecification of f are confirmed by the numerical experiments, these extensions are possible based on the current work, for instance, using a hierarchical approach for the number of objects. These are far from trivial and may depend on the specific application problems, and we here regard them as future directions.

The rest of the paper is organized as follows. The general results on the posterior contraction rate, along with the examples when applying specific priors are given in Section 3. We next focus on the most important case $d = 2$, and use the rescaled SE Gaussian process on \mathbb{S}^1 as the prior. We study the corresponding RKHS in Section 4, heavily relying on the properties of modified Bessel functions of the first kind. We also show that the posterior contraction rate of the boundary is nearly minimax-optimal, which is $n^{-\alpha/(\alpha+1)}$ up to a logarithmic factor, adaptively to the smoothness level α of the boundary. Section 5 proposes an efficient Markov Chain Monte Carlo methods for computing the posterior distribution of the boundary using the randomly rescaled Gaussian process prior, for various noise distributions. Section 6 studies the performance of the proposed Bayesian estimator via simulations, under various settings for both binary images and Gaussian noised images. Section 7 contains proofs to all theorems and lemmas. Section 8 provides several new results on the modified Bessel functions of the first kind.

2. Model and Notations. We consider a d -dimensional image $(X_i, Y_i)_{i=1}^n$ for $d = 2, 3, \dots$, where X_i is the location of the i th observa-

tion and Y_i is the image intensity. We consider the locations within the d -dimensional unit hypercube $T = [-1/2, 1/2]^d$ without loss of generality. Depending on the scheme of collecting data, we have the following options for the distribution P_{X_i} of X_i :

- *Completely Random Design.* $X_i \stackrel{i.i.d.}{\sim} \text{Uniform}(T)$.
- *Jitteredly Random Design.* Let T_i be the i th pixel when partitioning T into grids. Then X_i is chosen randomly at T_i , i.e. $X_i \sim \text{Uniform}(T_i)$ independently.

The region Γ is assumed to be star-shaped with a known or easily detectable reference point, and hence we may assume that the origin O is inside Γ without loss of generality, i.e. $O \in \Gamma$ and the boundary $\gamma = \partial\Gamma$ is a $(d-1)$ -dimensional closed manifold and has smoothness α which is made precise below. In view of a converse of the Jordan curve theorem we represent the closed boundary γ as a function indexed by \mathbb{S}^{d-1} , i.e. $\gamma : \mathbb{S}^{d-1} \rightarrow \mathbb{R}^+ : s \rightarrow \gamma(s)$. We further assume that the boundary γ is α -smooth, i.e. $\gamma \in \mathbb{C}^\alpha(\mathbb{S}^{d-1})$, where $\mathbb{C}^\alpha(\mathbb{S}^{d-1})$ is the α -Hölder class on \mathbb{S}^{d-1} . Specifically, let α_0 be the largest integer strictly smaller than α , then

$$\mathbb{C}^\alpha(\mathbb{S}^{d-1}) = \{f : \mathbb{S}^{d-1} \rightarrow \mathbb{R}^+, |f^{(\alpha_0)}(x) - f^{(\alpha_0)}(y)| \leq L_f \|x - y\|^{\alpha - \alpha_0} \\ \text{for } \forall x, y \in \mathbb{S}^{d-1} \text{ and some } L_f > 0\},$$

where $\|\cdot\|$ is the Euclidean distance. A different definition of smoothness was used by [28] based on the class of sets in [10], which cover cases of unsmooth boundary but with smooth parameterization. Here we focus on the class of smooth boundary therefore it may be more natural to use the definition of $\mathbb{C}^\alpha(\mathbb{S}^{d-1})$ directly.

We use θ to denote the triplet (ξ, ρ, γ) . Let ϕ_i be the parameters at the i th location, i.e. $\phi_i = \xi \mathbb{1}(X_i \in \Gamma) + \rho \mathbb{1}(X_i \in \Gamma^c)$ where $\mathbb{1}(\cdot)$ is the indicator function. The model assumes that $Y|X \sim P_\theta^n$ for some θ , where P_θ^n has density $\prod_{i=1}^n p_{\theta,i}(Y_i) = \prod_{i=1}^n f(Y_i; \phi_i)$ with respect to ν^n . Let

$$d_n^2(\theta, \theta') = \frac{1}{n} \sum_i \int (\sqrt{p_{\theta,i}} - \sqrt{p_{\theta',i}})^2 d\nu$$

be the average of the squares of the Hellinger distance for the distributions of the individual observations. Let $K(f, g) = \int f \log(f/g) d\nu$, $V(f, g) = \int f |\log(f/g)|^2 d\nu$, and $\|\cdot\|_p$ denote the L_p norm ($1 \leq p \leq \infty$). We use $f \lesssim g$ if there is an universal constant C such that $f \lesssim Cg$, and $f \asymp g$ if $f \lesssim g \lesssim f$. For a vector $x \in \mathbb{R}^d$, define $\|x\|_p = \{\sum_i |x_i|^p\}^{1/p}$ and $\|x\|_\infty = \max_{1 \leq i \leq p} |x_i|$. For two sets Γ and Γ' , we use $\Gamma \Delta \Gamma'$ for their symmetric difference and

$\lambda(\Gamma \triangle \Gamma')$ for its corresponding Lebesgue measure. We also use $\lambda(\gamma, \gamma')$ for $\lambda(\Gamma \triangle \Gamma')$ when $\gamma = \partial\Gamma$ and $\gamma' = \partial\Gamma'$. Observe that $\lambda(\gamma, \gamma') \lesssim \|\gamma - \gamma'\|_\infty$. For any $a, a' \in \mathbb{R}$, let $a \wedge a' = \min(a, a')$, and $a \vee a' = \max(a, a')$. For $\epsilon > 0$, define $\log_- \epsilon = 0 \vee \log(1/\epsilon)$.

3. Main results for the posterior convergence. In the following sections, we shall focus on the jitteredly random design; the completely random design is more straightforward and follows the same rate calculation with minor modifications. The likelihood function is given by

$$L(Y|X, \theta) = \prod_{i \in I_1} f(Y_i; \xi) \prod_{i \in I_2} f(Y_i; \rho),$$

where $I_1 = \{i : X_i \in \Gamma\}$ and $I_2 = \{i : X_i \in \Gamma^c\}$. The parameters $(\xi, \rho) \in \Theta^*$, where Θ^* is a subset of $\Theta \times \Theta = \{(\xi, \rho) : \xi \in \Theta, \rho \in \Theta\}$. The set Θ^* is typically given as the full parameter space $\Theta \times \Theta$ with some order restriction between ξ and ρ . For instance, when $f(\cdot)$ is the Bernoulli distribution, then $\Theta^* = \{(\xi, \rho) \in \mathbb{R}^2 : 0 < \rho < \xi < 1\}$ if the inside probability ξ is believed to be larger than the outside probability. We assume the distribution $f(\cdot)$ has the following regularity conditions:

- (A). For fixed ϕ_0 , we have $K(f(\cdot; \phi_0), f(\cdot; \phi)) \lesssim \|\phi - \phi_0\|^2$ and $V(f(\cdot; \phi_0), f(\cdot; \phi)) \lesssim \|\phi - \phi_0\|^2$ as $\|\phi - \phi_0\|^2 \rightarrow 0$;

The observations Y_i 's are conditionally independent given parameters. In the following sections, we let θ_0 denote the true value of the parameter vector $(\xi_0, \rho_0, \gamma_0)$ generating the data, and the corresponding region with boundary γ_0 is denoted by Γ_0 .

We shall denote the prior on θ by Π . By a slight abuse of notations, we denote the priors on (ξ, ρ) and γ also by Π . We next present the abstract forms of the required prior distributions in order to satisfy the minimax-optimal posterior contraction rate later on. The prior on (ξ, ρ) is independent with the prior on γ and satisfies that

- (B1). $\Pi(\xi, \rho)$ has a positive and continuous density on Θ^* ;
- (B2). Polynomial tails: there are some constants $t_1, t_2 > 0$ such that for any $M > 0$, we have $\Pi(\xi : \xi \notin [-M, M]^p) \leq t_1 M^{-t_1}$ and $\Pi(\rho : \rho \notin [-M, M]^p) \leq t_2 M^{-t_2}$.

The estimation and inference on γ is of main interest. Therefore (ξ, ρ) are considered as two nuisance parameters. When γ is modeled nonparametrically, the contraction rate for θ is primarily influenced by γ . The following condition is critical to relate $d_n(\theta, \theta')$ to $\lambda(\gamma, \gamma')$, which will lead to the contraction rate for γ .

- (C). For a fixed $(\xi_0, \rho_0) \in \Theta^*$, there exists a positive constant c_0 such that for arbitrary $(\xi, \rho) \in \Theta^*$, $h(f(\cdot; \xi_0), f(\cdot; \rho)) + h(f(\cdot; \rho_0), f(\cdot; \xi)) \geq c_0 > 0$, where $h(f(\cdot; \phi), f(\cdot; \phi'))$ is the Hellinger distance between the two densities $f(\cdot; \phi)$ and $f(\cdot; \phi')$.

Throughout this paper, we shall use $h(\phi, \phi')$ to abbreviate $h(f(\cdot; \phi), f(\cdot; \phi'))$.

Assumption (C) holds for most commonly used distribution families $\{f(\cdot; \phi); \phi \in \Theta\}$ when Θ^* considers the order restriction between ξ and ρ . Examples include but are not limited to:

- One-parameter family such as Bernoulli, Poisson, exponential distributions, and $\Theta^* = \Theta^2 \cap \{(\xi, \rho) : \rho < \xi\}$, or $\Theta^* = \Theta^2 \cap \{(\xi, \rho) : \rho > \xi\}$.
- Two-parameter family such as Gaussian distributions, and $\Theta^* = \Theta^2 \cap \{((\mu_1, \sigma_1), (\mu_2, \sigma_2)) : \mu_1 > \mu_2, \sigma_1 = \sigma_2\}$, or $\Theta^* = \Theta^2 \cap \{((\mu_1, \sigma_1), (\mu_2, \sigma_2)) : \mu_1 > \mu_2, \sigma_1 > \sigma_2\}$, or $\Theta^* = \Theta^2 \cap \{((\mu_1, \sigma_1), (\mu_2, \sigma_2)) : \mu_1 = \mu_2, \sigma_1 > \sigma_2\}$.

In practice, the order restriction is often naturally obtained depending on the concrete problems and facility to produce images. For instance, in brain oncology, a tumor often has higher intensity values than its surroundings in a positron emission tomography scan, while for astronomical applications objects of interest emit light and will be brighter. In this paper, we use the abstract condition (C) to provide a general framework for various relevant applications without assuming these specific subject matter restrictions. The following general theorem gives a posterior contraction rate for parameters θ and γ .

THEOREM 3.1. *Let a sequence ϵ_n such that $\epsilon_n \rightarrow 0$, $n\epsilon_n^2 \rightarrow \infty$, and $\log_- \epsilon_n^2 \lesssim n\epsilon_n^2$. Under Conditions (A), (B1), (B2), if there exists Borel measurable subsets $\Sigma_n \subset \mathbb{C}^\alpha(\mathbb{S}^{d-1})$ such that*

$$(3.1) \quad -\log \Pi(\gamma : \lambda(\Gamma_0 \triangle \Gamma) \leq \epsilon_n^2) \lesssim n\epsilon_n^2,$$

$$(3.2) \quad -\log \Pi(\gamma \in \Sigma_n^c) \gtrsim n\epsilon_n^2,$$

$$(3.3) \quad \log N(\epsilon_n^2, \Sigma_n, \|\cdot\|_\infty) \lesssim n\epsilon_n^2,$$

then for the entire parameter $\theta = (\xi, \rho, \gamma)$, we have that for every $M_n \rightarrow \infty$,

$$(3.4) \quad \mathbb{P}_{\theta_0}^{(n)} \Pi(\theta : d_n(\theta, \theta_0) \geq M_n \epsilon_n | X^{(n)}, Y^{(n)}) \rightarrow 0.$$

Further, if Condition (C) holds, then for the boundary γ , we have that for every $M_n \rightarrow \infty$,

$$(3.5) \quad \mathbb{P}_{\theta_0}^{(n)} \Pi(\gamma : \lambda(\gamma, \gamma_0) \geq M_n \epsilon_n^2 | X^{(n)}, Y^{(n)}) \rightarrow 0.$$

Equation (3.5) claims that if the rate for θ is ϵ_n , then the boundary γ has the rate ϵ_n^2 in terms of the discrepancy metric $\lambda(\cdot, \cdot)$ and can be faster than $n^{-1/2}$ which is another intriguing aspect of a boundary detection problem. In addition, it follows immediately that $\|\xi_0 - \xi\| \lesssim \epsilon_n$ and $\|\rho_0 - \rho\| \lesssim \epsilon_n$, although these two parameters are not of our interest and are actually estimable at $n^{-1/2}$ rate. In the next two subsections, we consider two general classes of priors suitable for applications of Theorem 3.1.

3.1. *Rescaled Gaussian process priors on \mathbb{S}^{d-1} .* We use a rescaled squared exponential Gaussian process (GP) to induce priors on γ . Specifically, let W be a GP with the squared exponential kernel function $K(t, t') = \exp(-\|t - t'\|^2)$, where $t, t' \in \mathbb{S}^{d-1}$ and $\|\cdot\|$ is the Euclidean distance. Let $W^a = (W_{at}, t \in \mathbb{S}^{d-1})$ be the scaled GP with scale $a > 0$, whose covariance kernel becomes $K_a(t, t') = \exp(-a^2\|t - t'\|^2)$. The rescaling factor a acts as a smoothing parameter and allows us to control smoothness of a sample path from the prior distribution .

The corresponding RKHS of a GP plays a critical role in calculating the posterior contraction rate. There has been an intensive study of the RKHS of a GP indexed by $[0, 1]^{d-1}$ [e.g. 41, 43]. These two GP's can be naturally related by a surjection $Q : [0, 1]^{d-1} \rightarrow \mathbb{S}^{d-1}$ (for example, using the spherical coordinate system). Define the following kernels on $[0, 1]^{d-1}$: $G(s_1, s_2) = K(Qs_1, Qs_2)$ for any $s_1, s_2 \in [0, 1]^{d-1}$. Let \mathbb{H} be the RKHS of the GP defined by the kernel K , equipped with the inner product $\langle \cdot, \cdot \rangle_{\mathbb{H}}$ and the RKHS norm $\|\cdot\|_{\mathbb{H}}$. For the GP defined by G , we define the corresponding counterparts using the notations \mathbb{H}' , $\langle \cdot, \cdot \rangle_{\mathbb{H}'}$ and $\|\cdot\|_{\mathbb{H}'}$ respectively. Then the following lemma shows that the two RKHS's related by the map Q are isomorphic.

LEMMA 3.2. *(\mathbb{H}' , $\|\cdot\|_{\mathbb{H}'}$) and (\mathbb{H} , $\|\cdot\|_{\mathbb{H}}$) are isometric; the conclusion also holds when we use the $\|\cdot\|_{\infty}$ norm.*

However, the kernel $G(\cdot, \cdot)$ (and also $G_a(\cdot, \cdot)$) is no longer a squared exponential kernel on $[0, 1]^{d-1}$. More importantly, it is not even stationary for general $d > 2$. The case $d = 2$ is an exception, for which the RKHS can be studied via an explicit treatment such as analytical eigen decompositions of its equivalent kernel on the unit interval; see Section 4.

3.2. *Rate calculation using finite random series priors.* The boundary γ_0 is a function on \mathbb{S}^{d-1} , which can be regarded also as a function on $[0, 1]^{d-1}$ with periodicity restrictions. We construct a sequence of finite dimensional approximation for functions in $\mathbb{C}^\alpha([0, 1]^{d-1})$ with periodicity restriction by

linear combinations of the first J elements of a collection of fixed functions to be called a basis. Let $\boldsymbol{\xi} = \boldsymbol{\xi}_J = (\xi_1, \dots, \xi_J)^T$ be the vector formed by the first J basis functions, and $\boldsymbol{\beta}_{0,J}^T \boldsymbol{\xi}$ be a linear approximation to γ_0 with $\|\boldsymbol{\beta}_{0,J}\|_\infty < \infty$. We assume that the basis functions satisfy the following condition:

$$(D). \quad \max_{1 \leq j \leq J} \|\xi_j\|_\infty \leq t_3 J^{t_4} \text{ for some constants } t_3, t_4 \geq 0.$$

This includes most commonly used basis functions, such as B-splines, Fourier series, polynomials and wavelets. We use the random series prior for γ by inducing a prior on $\boldsymbol{\beta}^T \boldsymbol{\xi}$ through the number of basis functions J and the corresponding coefficients $\boldsymbol{\beta}$ given J . For the simplicity of notations, we use $\boldsymbol{\beta}$ ($\boldsymbol{\beta}_0$) for $\boldsymbol{\beta}_J$ ($\boldsymbol{\beta}_{0,J}$) when J is explicit from the context.

Priors. Let Π stand for the probability mass function (p.m.f.) of J , and also for the prior for $\boldsymbol{\beta}$. We use a Poisson prior distribution on J and multivariate normal for $\boldsymbol{\beta}$, satisfying the general conditions in [39]:

$$(E1). \quad -\log \Pi(J > j) \gtrsim j \log j, \text{ and } -\log \Pi(J = j) \lesssim j \log j.$$

$$(E2). \quad -\log \Pi(\|\boldsymbol{\beta} - \boldsymbol{\beta}_0\|_1 \leq \epsilon | J) \lesssim J \log(1/\epsilon), \text{ and } \Pi(\boldsymbol{\beta} \notin [-M, M]^J | J) \leq J \exp\{-CM^2\} \text{ for some constant } C.$$

We derive conditions to obtain the posterior contraction rate as follows.

THEOREM 3.3. *Let ϵ_n be a sequence such that $\epsilon_n \rightarrow 0$ and $n\epsilon_n^2/\log n$ is bounded away from 0, and J_n be a sequence such that $J_n \rightarrow \infty$ and $J_n \leq n$. Under conditions (D), (E1) and (E2), if ϵ_n, J_n satisfy*

$$\|\gamma_0 - \boldsymbol{\beta}_{0,J_n}^T \boldsymbol{\xi}\|_\infty \leq \epsilon_n^2/2, \quad c_1 n \epsilon_n^2 \leq J_n \log J_n \leq J_n \log n \leq c_2 n \epsilon_n^2,$$

as $n \rightarrow \infty$ for some constants $c_1 > 0$ and $c_2 > 0$, then equation (3.5) hold, i.e. ϵ_n^2 is the posterior contraction rate for γ in terms of the distance $\lambda(\cdot, \cdot)$.

REMARK 3.4. The optimal value of J_n , say $J_{n,\alpha}$ typically depends on the degree of smoothness α . We can use a fixed value $J = J_n$ when α is given. The posterior distribution can be easily computed, for example, by a Metropolis-Hastings algorithm. If α is unknown, one will need to put a prior on J and the reversible-jump MCMC may be needed for computation.

EXAMPLE 3.5 (Trigonometric polynomials). For the case $d = 2$ (2D image), we use trigonometric polynomials $\{1, \cos 2\pi j\omega, \sin 2\pi j\omega, \dots, \omega \in [0, 1]\}$ as the basis, which is . It is known that for some appropriately choice of $\boldsymbol{\beta}_{0,j}$, $\|\gamma_0 - \boldsymbol{\beta}_{0,j}^T \boldsymbol{\xi}\|_\infty \lesssim j^{-\alpha}$ [cf. 19] if γ is α -smooth. Therefore from Theorem 3.3, we can obtain the rate ϵ_n by equating $J_n^{-\alpha} \asymp \epsilon_n^2$ and $J_n \log J_n \asymp n \epsilon_n^2$,

which gives the following rate ϵ_n and the corresponding J_n :

$$J_n \asymp n^{1/(\alpha+1)}(\log n)^{-1/(\alpha+1)}, \quad \epsilon_n^2 \asymp n^{-\alpha/(\alpha+1)}(\log n)^{\alpha/(\alpha+1)}.$$

EXAMPLE 3.6 (Spherical harmonics). For 3D images ($d = 3$), periodic functions on the sphere can be expanded in the spherical harmonic basis functions. Spherical harmonics are eigenfunctions of the Laplacian on the sphere. It satisfies condition (D) and more technical details and the analytical expressions of spherical harmonics can be found in [40, Chapter 2], while MATLAB implementation is available in [11]. Let K_n be degree of the spherical harmonics, then the number of basis functions are $J_n = K_n^2$. The approximation error for spherical harmonics is $J_n^{-\alpha/2}$ [8, Theorem 4.4.2]. Therefore we can obtain the posterior contraction rate by equating $J_n^{-\alpha/2} \asymp \epsilon_n^2$ and $J_n \log J_n \asymp n\epsilon_n^2$, which gives

$$J_n \asymp n^{2/(\alpha+2)}(\log n)^{-2/(\alpha+2)}, \quad \epsilon_n^2 \asymp n^{-\alpha/(\alpha+2)}(\log n)^{\alpha/(\alpha+2)}.$$

4. Squared exponential periodic kernel GP. When $d = 2$, it is natural to use the map $Q : [0, 1] \rightarrow \mathbb{S}^1, \omega \rightarrow (\cos 2\pi\omega, \sin 2\pi\omega)$ as in [27], then by Lemma 3.2, the squared exponential kernel $K_a(\cdot, \cdot)$ on \mathbb{S}^1 has the equivalent RKHS as of the kernel $G_a(t_1, t_2)$ on $[0, 1]$ defined by $G_a(t_1, t_2) = \exp(-a^2\{(\cos 2\pi t_1 - \cos 2\pi t_2)^2 + (\sin 2\pi t_1 - \sin 2\pi t_2)^2\}) = \exp\{-4a^2 \sin^2(\pi t_1 - \pi t_2)\}$. We call $G_a(\cdot, \cdot)$ on the unit interval as *squared exponential periodic* (SEP) kernel. It is stationary since $G_a(t_1, t_2) = \phi_a(t_1 - t_2)$, where $\phi_a(t) = \exp\{-4a^2 \sin^2(\pi t)\}$. In the next two subsections, we study the RKHS of a GP $W^a = \{W_t^a : t \in [0, 1]\}$ with the SEP kernel $G_a(\cdot, \cdot)$ and propose an adaptive Bayesian estimation procedure for the discussed boundary detection problem. Throughout the paper, the rescaling factor $a > 0$.

4.1. *RKHS under rescaling.* The following result gives the explicit form of the spectral measure μ_a of the process W_t^a . Let δ_x be the Kronecker delta function and $I_n(x)$ be the modified Bessel function of the first kind with order n and argument x where $n \in \mathbb{Z}$ and $x \in \mathbb{R}$.

LEMMA 4.1. *We have $\phi_a(t) = \int e^{-its} d\mu_a(s)$, where μ_a is a symmetric and finite measure and given by $\mu_a = \sum_{n=-\infty}^{\infty} e^{-2a^2} I_n(2a^2) \delta_{2\pi n}$.*

In addition, the Karhunen-Loève expansion of the covariance kernel is $G_a(t, t') = \sum_{k=1}^{\infty} v_k(a) \psi_k(t) \psi_k(t')$, where the eigenvalues $v_k(a)$'s are $v_1(a) = e^{-2a^2} I_0(2a^2)$, $v_{2j}(a) = v_{2j+1}(a) = e^{-2a^2} I_j(2a^2)$, $j \geq 1$, and eigenfunctions $\psi_k(t)$'s are the Fourier basis functions $\{1, \cos 2\pi t, \sin 2\pi t, \dots\}$.

The measure μ_a is the so-called spectral measure of W^a . Existing literature [e.g. 41, 43] studied convergence properties of rescaled GP on $[0, 1]^{d-1}$ relying on the absolute continuity of the according spectral measure and $\mu_a(B) = \mu_1(aB)$. However, Lemma 4.1 indicates that the spectral measure of a SEP Gaussian process is discrete and the simple relationship $\mu_a(B) = \mu_1(aB)$ does not hold any more. We instead heavily use properties of modified Bessel functions to study the RKHS of a SEP Gaussian process.

Note that the discrete measure μ_a has subexponential tails since

$$\int e^{|s|} \mu_a(ds) = \sum_{n=-\infty}^{\infty} e^{2\pi|n|} e^{-2a^2} I_n(2a^2) \leq 2 \sum_{n=-\infty}^{\infty} e^{-2a^2} I_n(2a^2)$$

which is $2e^{a^2(e^{2\pi} + e^{-2\pi})} < \infty$ (Proposition 8.1 (a)). The following Lemma 4.2 describes the RKHS \mathbb{H}^a of the rescaled process W^a .

LEMMA 4.2. \mathbb{H}^a is the set of real parts of all functions in

$$\begin{aligned} \{h : [0, 1] \rightarrow \mathbb{C}, h(t) = \sum_{n=-\infty}^{\infty} e^{-it2\pi n} b_{n,a} e^{-2a^2} I_n(2a^2), \\ b_{n,a} \in \mathbb{C}, \sum_{n=-\infty}^{\infty} |b_{n,a}|^2 e^{-2a^2} I_n(2a^2) < \infty\}, \end{aligned}$$

and it is equipped with the squared norm

$$\|h\|_{\mathbb{H}^a}^2 = \sum_{n=-\infty}^{\infty} |b_{n,a}|^2 e^{-2a^2} I_n(2a^2) = \sum_{n=-\infty}^{\infty} \frac{1}{e^{-2a^2} I_n(2a^2)} \left| \int_0^1 h(t) e^{it2\pi n} dt \right|^2.$$

We then consider the approximation property of \mathbb{H}^a to an arbitrary smooth function $w \in \mathbb{C}^\alpha[0, 1]$. Unlike the approach approximating w by a convolution of w_0 with a smooth function as used in [41, 43], we use a finite Fourier approximation to w .

LEMMA 4.3. For any function $w \in \mathbb{C}^\alpha[0, 1]$, there exists constants C_w and D_w depending only on w such that $\inf\{\|h\|_{\mathbb{H}^a}^2 : \|w - h\|_\infty \leq C_w a^{-\alpha}\} \leq D_w a$, as $a \rightarrow \infty$.

Lemma 4.4 obtains an entropy estimate using Proposition 8.3 on modified Bessel functions.

LEMMA 4.4. Let \mathbb{H}_1^a be the unit ball of the RKHS of the process $W^a = (W_t^a : 0 \leq t \leq 1)$, then we have $\log N(\epsilon, \mathbb{H}_1^a, \|\cdot\|_\infty) \lesssim \max(a, 1) \cdot \{\log(1/\epsilon)\}^2$.

As a corollary of Lemma 4.4, using the connection between the entropy of the unit ball of the RKHS and the small ball probability [24, 25], we have the following estimate of the small ball probability.

LEMMA 4.5 (Lemma 4.6 in [43]). *For any $a_0 > 0$, there exists constants C and ϵ_0 that depend only on a_0 such that, for $a \geq a_0$ and $\epsilon \leq \epsilon_0$,*

$$-\log \mathbb{P} \left(\sup_{0 \leq t \leq 1} |W_t^a| \leq \epsilon \right) \leq Ca \left(\log \frac{a}{\epsilon} \right)^2.$$

4.2. *Contraction rate for deterministic rescaling.* Assume the smoothness level parameter α is known. Let \mathbb{B} be $\mathbb{C}^\alpha(\mathbb{S}^1)$ equipped with the $\|\cdot\|_\infty$ norm. Let $\phi_{\gamma_0}^a(\epsilon) = \inf_{\gamma \in \mathbb{H}^a: \|\gamma - \gamma_0\|_\infty \leq \epsilon} \frac{1}{2} \|\gamma\|_{\mathbb{H}^a}^2 - \log \mathbb{P}(\|W^a\|_\infty \leq \epsilon)$ stand for the concentration function at γ_0 . Note that $\phi_0^a(\epsilon) = -\log \mathbb{P}(\|W^a\|_\infty \leq \epsilon)$.

The selection of sieves and entropy calculation is similar to Theorem 2.1 in [42] with ϵ_n replaced by ϵ_n^2 as follows. Define the sieve as $\Sigma_n = (M_n \mathbb{H}_1^a + \epsilon_n^2 \mathbb{B}_1)$, where \mathbb{H}_1^a and \mathbb{B}_1 are the unit balls of \mathbb{H}^a and \mathbb{B} respectively. Let $M_n = -2\Phi^{-1}(\exp(-Cn\epsilon_n^2))$ for a large constant $C > 1$. Then by Borell's inequality, we can bound $\Pi(\Sigma_n^c) \leq \Pi(\gamma \notin M_n \mathbb{H}_1^a + \epsilon_n^2 \mathbb{B}_1) \lesssim \exp(-Cn\epsilon_n^2)$, provided that $\phi_0^a(\epsilon_n^2) \leq n\epsilon_n^2$.

For the entropy calculation, first observe that $M_n^2 \lesssim n\epsilon_n^2$ since $|\Phi^{-1}(u)| \leq \sqrt{2 \log(1/u)}$ for $u \in (0, 1/2)$. Therefore, according to Lemma 4.4, we have

$$\begin{aligned} \log N(3\epsilon_n^2, \Sigma_n, \|\cdot\|_\infty) &\leq \log N(2\epsilon_n^2, M_n \mathbb{H}_1^a, \|\cdot\|_\infty) = \log N \left(\frac{2\epsilon_n^2}{M_n}, \mathbb{H}_1^a, \|\cdot\|_\infty \right) \\ &\lesssim a \left(\log \frac{M_n}{2\epsilon_n^2} \right)^2 \lesssim a(\log n)^2. \end{aligned}$$

To evaluate the prior concentration probability, we proceed as follows. By the approximation property of \mathbb{H}^a in Lemma 4.3, there exists $h_0 \in \mathbb{H}^a$ such that $\|h_0 - \gamma_0\|_\infty \lesssim a^{-\alpha}$ and $\|h_0\|_{\mathbb{H}^a}^2 \lesssim a^{d-1}$. Therefore, if $a^{-\alpha} \leq \epsilon_n^2/2$, then

$$\Pi(\gamma : \|\gamma - \gamma_0\|_\infty \leq \epsilon_n^2) \geq \Pi(\gamma : \|\gamma - h_0\|_\infty \leq \epsilon_n^2/2) \geq \exp\{-\phi_0^a(\epsilon_n^2/4)\},$$

leading to $-\log \Pi(\gamma : \|\gamma - \gamma_0\|_\infty \leq \epsilon_n^2) \lesssim \phi_0^a(\epsilon_n^2/4)$.

Note that $\phi_0^a(\epsilon) \lesssim a(\log(a/\epsilon))^2$ (Lemma 4.5). To satisfy the conditions in Theorem 3.1, we choose $a = a_n$ depending on the sample size such that $\epsilon_n^2 \asymp a_n^{-\alpha}$, and $a_n(\log n)^2 \asymp n\epsilon_n^2$. Then the posterior contraction rate is obtained as $\epsilon_n^2 = n^{-\alpha/(\alpha+1)}(\log n)^{-2\alpha/(\alpha+1)}$, with $a_n = n^{1/(\alpha+1)}(\log n)^{-2/(\alpha+1)}$.

4.3. *Contraction rate for random rescaling.* When the underlying smoothness level α is unknown, the Gaussian process prior can adapt to α in a hierarchical Bayesian approach by assigning the rescaling parameter an appropriate prior such as a gamma distribution [43].

THEOREM 4.6. *If we use a rescaled SEP Gaussian process prior for γ and the rescaling factor follows a gamma prior, then the contraction rate in Theorem 3.1 is $\epsilon_n^2 = n^{-\alpha/(\alpha+1)}$ up to a logarithmic factor for any $\alpha > 0$.*

The proof of Theorem 4.6 needs a nesting property of the RKHS of W^a for different values of a . Lemma 4.7 in [43] proved that $\sqrt{a}\mathbb{H}_1^a \subset \sqrt{b}\mathbb{H}_1^b$ if $a \leq b$ for a squared exponential GP indexed by $[0, 1]^{d-1}$. For the SEP Gaussian process prior, this does not hold but can be modified up to a global constant.

LEMMA 4.7. *If $a \leq b$, then $\sqrt{a}\mathbb{H}_1^a \subset \sqrt{cb}\mathbb{H}_1^b$ for a universal constant c .*

When $a \downarrow 0$, sample paths of W^a tend to concentrate to a constant value by the following lemma. This property is crucial in controlling the variation of sample paths for small a .

LEMMA 4.8. *For $h \in \mathbb{H}_1^a$, we have $|h(0)| \leq 1$ and $|h(t) - h(0)| \leq 2\sqrt{2\pi}at$ for every $t \in [0, 1]$.*

5. Sampling Algorithms. We assume that the origin (center of the image) is inside the boundary, and thus use it as the reference point to represent the observed image in a polar coordinate system as $(\omega, \mathbf{r}; \mathbf{Y})$, where (ω, \mathbf{r}) are the locations using polar coordinates and \mathbf{Y} is the image intensity. Let γ be a closed curve, and γ be values of γ evaluated at each ω .

For most kernels, the eigenfunctions and eigenvalues are challenging to obtain although there are several exceptions [37, Ch. 4.3]. Therefore a randomly rescaled GP prior may be infeasible in practice since the numerical inversion of a covariance matrix is often needed when no analytical forms are available. However, thanks to the analytical eigen decomposition the SEP kernel in Lemma 4.1, we can implement this theoretically appealing prior in an computationally efficient way. If a curve $\gamma(\omega) \sim \text{GP}(\mu(\omega), G_a(\cdot, \cdot)/\tau)$, we then have the equivalent representation $\gamma(\omega) = \mu(\omega) + \sum_{k=1}^{\infty} z_k \psi_k(\omega)$, where $z_k \sim N(0, v_k(a)/\tau)$ independently.

The modified Bessel function of the first kind used in $v_k(a)$'s is a library function in most software, such as `besselI` in R language. Figure 1(a) shows that eigenvalues decay very fast when $a = 1, 10$. When a increases, the smoothness level of the kernel decreases. In practice we typically do not

use values as large as 100 since then the kernel becomes very close to the identity matrix and thus the resulting prior path becomes very rough. The fast decay rate guarantees that some suitable finite order truncation to the Karhunen-Loève expansion is able to approximate the kernel function well. Suppose we use $L = 2J + 1$ basis functions, then the truncated process is given by $\gamma(\omega) = \sum_{k=1}^L z_k \psi_k(\omega) + \mu(\omega)$. Figure 1(b) shows that with $J = 10$, we are able to explain at least 98% of all the variability for a reasonable range of a 's from 0 to 10.

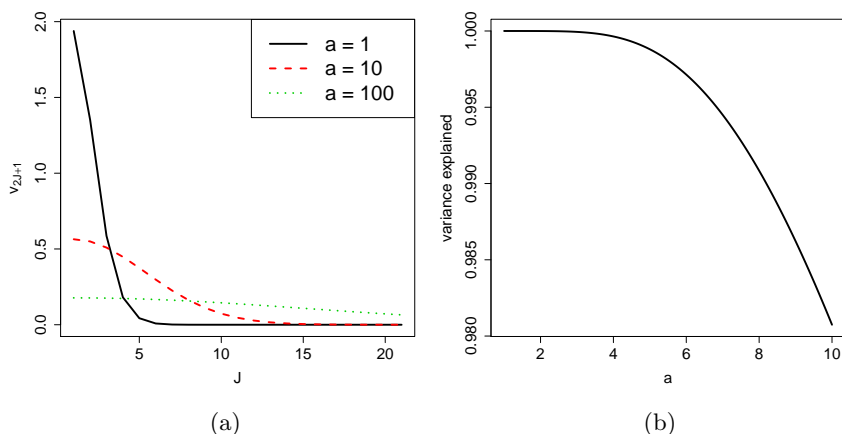


Fig 1: Decay rate of the eigenvalues of the squared exponential kernel. Figure (a) plots the values of $v_{2J+1}(a)$ at $J = 0, \dots, 20$ when $a = 1, 10, 100$. Figure (b) plots the proportion of the variance explained if using the first 21 ($J = 10$) basis functions at different values of a .

Let Ψ be the n by L matrix with the k th column comprising of the evaluations of $\psi_k(\cdot)$ at the components of ω , and μ comprising of the evaluations of $\mu(\cdot)$ at the components of ω . Then the Gaussian process prior for the boundary curve can be expressed as

$$\gamma = \Psi z + \mu; \quad z \sim N(0, \Sigma_a / \tau)$$

where $\Sigma_a = \text{diag}(v_1(a), \dots, v_L(a))$. We use the following priors for the hyperparameters involved in the covariance kernel: $\tau \sim \text{Gamma}(500, 1)$ and $a \sim \text{Gamma}(2, 1)$. For the mean $\mu(\cdot)$, we use a constant 0.1. Note that here we also can use empirical Bayes to estimate the prior mean by any ordinary one dimensional change-point method and an extra step of smoothing. However,

our numerical investigation shows that our method is robust in terms of the specification of $\mu(\cdot)$, which makes little difference on the performance.

The priors for (ξ, ρ) depend on the error distributions. We also need to use the order information between the parameters to keep the two regions distinguishable. We use OIB, OIN, OIG for ordered independent Bernoulli, normal and gamma distributions respectively. If not specified explicitly, the parameters are assumed to be in a decreasing order. It is easy to see that this convention is for simplicity of notations, and any order between the two region parameters are allowed in practice. We below give the conjugate priors for (ξ, ρ) for some commonly used noise distributions:

- Binary images: the parameters are the probabilities $(\pi_1, \pi_2) \sim \text{OIB}(\alpha_1, \beta_1, \alpha_1, \beta_1)$;
- Gaussian noise: the parameters are the mean and standard deviation $(\mu_1, \sigma_1, \mu_2, \sigma_2)$ with the priors to be $(\mu_1, \mu_2) \sim \text{OIN}(\mu_0, \sigma_0^2, \mu_0, \sigma_0^2)$ and $(\sigma_1^{-2}, \sigma_2^{-2}) \sim \text{OIG}(\alpha_2, \beta_2, \alpha_2, \beta_2)$.
- Poisson noise: the parameters are the rates $(\lambda_1, \lambda_2) \sim \text{OIG}(\alpha_3, \beta_3, \alpha_3, \beta_3)$;
- Exponential noise: the parameters are the rates $(\lambda_1, \lambda_2) \sim \text{OIG}(\alpha_4, \beta_4, \alpha_4, \beta_4)$.

In fact, any error distributions with conjugacy properties conditionally on the boundary can be directly used. The hyper-parameters (α, β) are not influential, and we can use values such that the distribution spread out or even improper priors. For example, in the simulation, we use $\alpha_1 = \beta_1 = 0$ for binary images; we use $\mu_0 = \bar{y}, \sigma_0 = 10^3$ and $\alpha_2 = \beta_2 = 10^{-2}$ for Gaussian noise.

We use the slice sampling technique [30] within the Gibbs sampler to draw samples from the posterior distribution for $(\mathbf{z}, \xi, \rho, \tau, a)$. Below is a detailed description of the sampling algorithms for binary images.

1. Initialize the parameters to be $\mathbf{z} = \mathbf{0}, \tau = 500$ and $a = 1$. The parameters $(\xi, \rho) = (\pi_1, \pi_2)$ are initialized by the maximum likelihood estimates (MLE) given the boundary to be $\mu(\cdot)$.
2. $\mathbf{z} | (\pi_1, \pi_2, \tau, a, \mathbf{Y})$: the conditional posterior density of \mathbf{z} (in a logarithmic scale and up to an additive constant) is equal to

$$\begin{aligned} & \sum_{i \in I_1} \log f(Y_i; \pi_1) + \sum_{i \in I_2} \log f(Y_i; \pi_2) - \frac{\tau \mathbf{z}^T \boldsymbol{\Sigma}_a^{-1} \mathbf{z}}{2} \\ & = N_1 \log \frac{\pi_1(1 - \pi_2)}{\pi_2(1 - \pi_1)} + n_1 \log \frac{1 - \pi_1}{1 - \pi_2} - \frac{\tau \mathbf{z}^T \boldsymbol{\Sigma}_a^{-1} \mathbf{z}}{2}, \end{aligned}$$

where $n_1 = \sum_i \mathbb{1}(r_i < \gamma_i)$ and $N_1 = \sum_i \mathbb{1}(r_i < \gamma_i)Y_i$. We use slice sampling one-coordinate-at-a-time for this step.

3. $\tau | (\mathbf{z}, a) \sim \text{Gamma}(a^*, b^*)$, where $a^* = a + L/2$ and $b^* = b + \mathbf{z}^T \boldsymbol{\Sigma}_a^{-1} \mathbf{z} / 2$;
4. $(\pi_1, \pi_2) | (\mathbf{z}, \mathbf{Y}) \sim \text{OIB}(\alpha_1 + N_1, \beta_1 + n_1 - N_1, \alpha_1 + N_2, \beta_1 + n_2 - N_2)$, where N_2 is the count of 1's outside γ and n_2 is the number of observations outside γ .
5. $a | \mathbf{z}, \tau$: use slice sampling by noting that the conditional posterior density of a (in a logarithmic scale and up to an additive constant) is equal to

$$-\frac{\log |\boldsymbol{\Sigma}_a|}{2} - \frac{\tau \mathbf{z}^T \boldsymbol{\Sigma}_a^{-1} \mathbf{z}}{2} + \log(ae^{-a}) = -\sum_{k=1}^L \frac{\log c_k}{2} - \sum_{k=1}^L \frac{\tau z_k^2}{2c_k} + \log a - a$$

The above algorithm is generic beyond binary images. For other noise distributions, the update of τ and a are the same. The update of \mathbf{z} and (ξ, ρ) in Step 2 and Step 4 will be changed using the corresponding priors and conjugacy properties. For example, for Gaussian noise, the parameters (ξ, ρ) are $(\mu_1, \sigma_1, \mu_2, \sigma_2)$, and the conditional posterior density (in a logarithmic scale and up to an additive constant) used in Step 2 is changed to

$$-n_1(\log \sigma_1 - \log \sigma_2) - (2\sigma_1^2)^{-1} \sum_{i \in I_1} (y_i - \mu_1)^2 - (2\sigma_2^2)^{-1} \sum_{i \in I_2} (y_i - \mu_2)^2 - \frac{\tau \mathbf{z}^T \boldsymbol{\Sigma}_a^{-1} \mathbf{z}}{2}.$$

For Step 4, the conjugacy is changed to

$$(\mu_1, \mu_2) | (\mathbf{z}, \sigma_1, \sigma_2, \mathbf{Y}) \sim \text{OIN}, \quad (\sigma_1^{-2}, \sigma_2^{-2}) | (\mathbf{z}, \mu_1, \mu_2, \mathbf{Y}) \sim \text{OIG}.$$

Similarly, it is straightforward to apply this algorithm to images with Poisson noise, exponential noise or other families of distributions with ordered conjugate prior.

6. Simulations.

6.1. *Numerical results for binary images.* We use jitteredly random design for locations $(\boldsymbol{\omega}, \mathbf{r})$ and three cases for boundary curves:

- Case B1. Ellipse given by $r(\omega) = b_1 b_2 / \sqrt{(b_2 \cos \omega)^2 + (b_1 \sin \omega)^2}$, where $b_1 \geq b_2$ and ω is the angular coordinate measured from the major axis. We set $b_1 = 0.35$ and $b_2 = 0.25$.
- Case B2. Ellipse with shift and rotation: centered at $(0.1, 0.1)$ and rotated by 60° counterclockwise. We use this setting to investigate the influence of the specification of the reference point.

- Case B3. Regular triangle centered at the origin with the height to be 0.5. We use this setting to investigate the performance of our method when the true boundary is not smooth at some points.

We keep using $\pi_2 = 0.2$ and vary the values of π_1 to be $(0.5, 0.25)$. For each combination of (π_1, π_2) , we use $m = 100, 500$ (recall that $n = m^2$). The MCMC procedure is iterated 5,000 times after 1,000 steps burn-in period. For the estimates, we calculate the Lebesgue error (area of mismatched regions) between the estimates and the true boundary. For the proposed Bayesian approach, we use the posterior mean as the estimate and construct a variable-width uniform credible band. Specifically, let $\{\gamma_i(\omega)\}_{1000}^{5000}$ be the posterior samples and $(\hat{\gamma}(\omega), \hat{s}(\omega))$ be the posterior mean and standard deviation functions derived from $\{\gamma_i(\omega)\}$. For each MCMC run, we calculate the distance $u_i = \|(\gamma_i - \hat{\gamma})/s\|_\infty = \sup_\omega \{|\gamma_i(\omega) - \hat{\gamma}(\omega)|/\hat{s}(\omega)\}$ and obtain the 95th percentile of all the u_i 's, denoted as L_0 . Then a 95% uniform credible band is given by $[\hat{\gamma}(\omega) - L_0\hat{s}(\omega), \hat{\gamma}(\omega) + L_0\hat{s}(\omega)]$.

We compare the proposed approach with a maximum contrast estimator (MCE) which first detect boundary pixels followed by a post-smoothing via a penalized Fourier regression. In the 1-dimensional case, the MCE selects the location which maximizes the differences of the parameter estimates at the two sides, which is similar to many pixel boundary detection algorithms discussed in [32]. In images, for a selected number of angles (say 1000 equal-spaced angles from 0 to 2π), we choose the neighboring bands around each angle and apply MCE to obtain the estimated radius and then smooth those estimates via a penalized Fourier regression. Note that unlike the proposed Bayesian approach, a joint confidence band is not conveniently obtainable for the method of MCE, due to its usage of a two-step procedure.

As indicated by Table 1, the proposed Bayesian method has Lebesgue errors typically less than 2.5%. In addition, the proposed method outperforms the benchmark method MCE significantly. We also observe that the MCE method is highly affected by the number of basis functions; in contrast, the proposed method adapts to the smoothness level automatically. The comparison between Case B1 and Case B2 shows that the specification of the reference point will not influence the performance of our methods since the differences are not significant compared to the standard error.

Figures 2 and 3 confirm the superior performance of the proposed method compared with the smoothed MCE method with 5 and 31 basis functions when the true boundary curve is an ellipse, an ellipse with shift and rotation and a triangle. Even in the case of $\pi_1 = 0.25$ where the contrast at two sides of the boundary is small, the proposed method is still able to capture the boundary when $m = 500$. This observation is consistent with the result

TABLE 1
Lebesgue errors ($\times 10^{-2}$) of the methods based on 100 simulations. The standard errors are reported below in the parentheses.

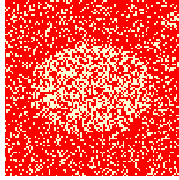
	$m = 100, (\pi_1, \pi_2) = (0.50, 0.20)$			$m = 100, (\pi_1, \pi_2) = (0.25, 0.20)$		
	Case B1	Case B2	Case B3	Case B1	Case B2	Case B3
Bayesian method	0.64 (0.02)	0.67 (0.02)	2.26 (0.02)	0.71 (0.03)	0.8 (0.03)	2.36 (0.03)
MCE with 5 bases	6.57 (0.25)	6.58 (0.21)	6.03 (0.07)	6.39 (0.19)	10.09 (0.20)	7.03 (0.11)
MCE with 31 bases	8.75 (0.18)	7.84 (0.19)	5.96 (0.10)	9.19 (0.16)	11.8 (0.19)	7.86 (0.14)

derived from the infill asymptotics. In addition, we also obtain joint credible bands using the samples drawn from the joint posterior distribution.

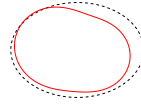
6.2. *Numerical results for Gaussian noised images.* For Gaussian noised images, we keep using an ellipse with shift and rotation as the true boundary curve (i.e. Case B2). We consider the following four scenarios where the two standard deviations are all given by $(\sigma_1, \sigma_2) = (1.5, 1)$ and the observed image is 100×100 :

- Case G1. $\mu_1 = 4, \mu_2 = 1$, i.e. the two regions differ in both the first two moments;
- Case G2. $\mu_1 = \mu_2 = 1$, i.e. the two regions only differ in the standard deviation;
- Case G3. (μ_1, μ_2) are functions of the location. Let r^I be the smallest radius inside the boundary, and r^O the largest radius outside the boundary. We use $\mu(i)$ for the mean of Y_i and let $\mu(i) = r_i - r^I + 0.2$ if it is inside, while $\mu(i) = r_i + r^O$ if outside. Therefore, the mean values vary at each location but have a gap of 0.2 between the two regions.
- Case G4. We use mixture normal distribution $0.6N(2, \sigma_1^2) + 0.4N(1, \sigma_2^2)$ for the inside distribution; the outside distribution is still Gaussian with mean $\mu_2 = 1$.

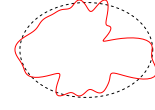
Cases G3 and G4 allow us to investigate the performance of the proposed method when the distribution $f(\cdot)$ in the model is misspecified. For comparison, we use a 1-dimensional change-point detection algorithm [6, 22] via the R package `changepoint` [21]. For the post-smoothing step, we use a penalized Fourier regression with 5 and 31 basis functions (method CP5 and CP31 in Table 2). Here we use the estimates of CP5 as the mean in the Gaussian process prior. Table 2 shows that the proposed method has good performance for all the four cases. The method of CP5 and CP10 produce small errors in Case G1, but suffer a lot from the other three cases. It shows

(a) Ellipse ($m = 100$, $\pi_1 = 0.50$)

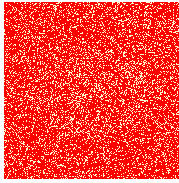
(b) Bayesian Est.



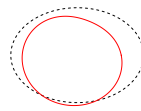
(c) MCE (5 basis)



(d) MCE (31 basis)

(e) Ellipse ($m = 500$, $\pi_1 = 0.25$)

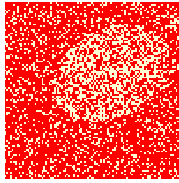
(f) Bayesian Est.



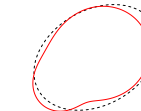
(g) MCE (5 basis)



(h) MCE (31 basis)

(i) Ellipse with shift and rotation ($m = 100$, $\pi_1 = 0.50$)

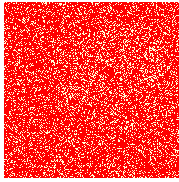
(j) Bayesian Est.



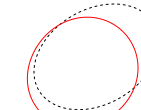
(k) MCE (5 basis)



(l) MCE (31 basis)

(m) Ellipse with shift and rotation ($m = 500$, $\pi_1 = 0.25$)

(n) Bayesian Est.



(o) MCE (5 basis)



(p) MCE (31 basis)

Fig 2: Performance on binary images (Column 1) with elliptic boundary. Column 2–4 plot the estimate (solid line in red) against the true boundary (dotted line in black). A 95% uniform credible band (in gray) is provided for the Bayesian estimate (Column 2).

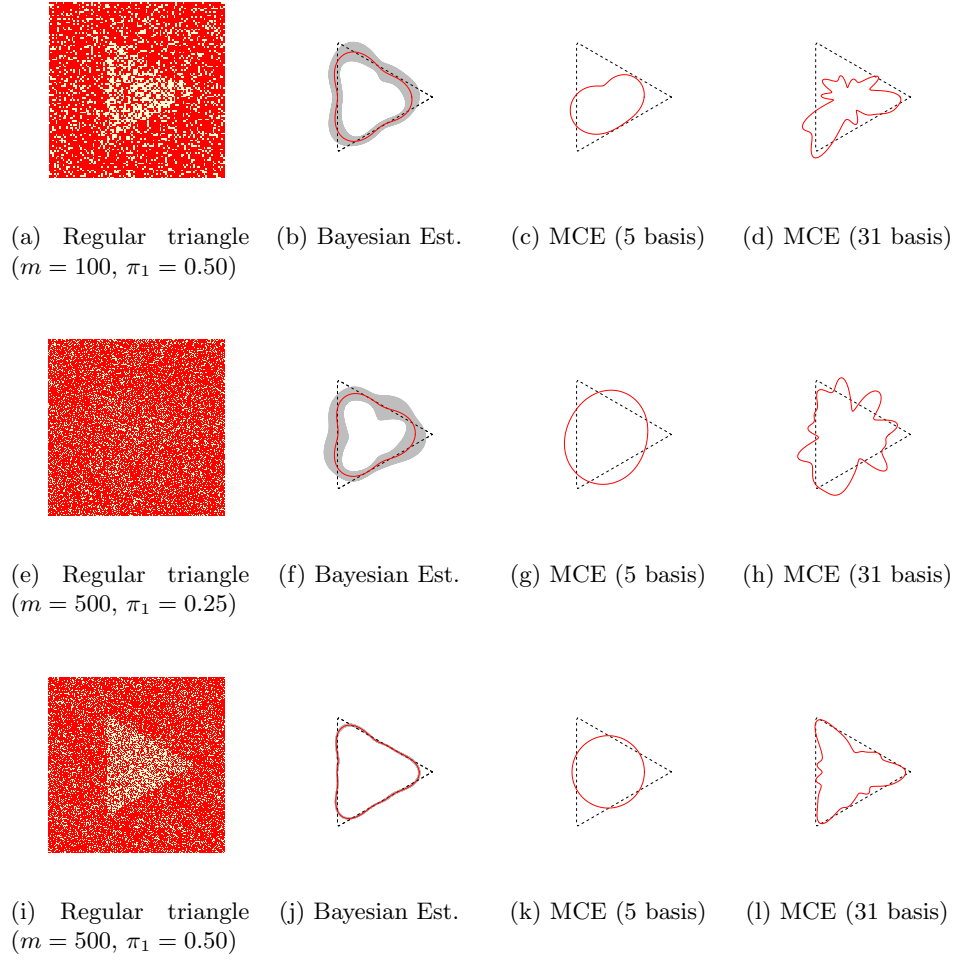


Fig 3: Performance on binary images (Column 1) when the boundary curve is an regular triangle. Column 2–4 plot the estimate (solid line in red) against the true boundary (dotted line in black). A 95% uniform credible band (in gray) is provided for the Bayesian estimate (Column 2).

that the change-point method highly depends on the distinction between the means (Case G2), and also it loses its way when the model is misspecified. In fact, for Cases G2, G3 and G4, the CP5 and CP31 methods lead to a curve almost containing the whole frame of the image. The proposed Bayesian approach which models the boundary directly, seems to be not affected even when the model is substantially misspecified (Case G3). Figure 4 shows the noisy observation and our estimation from 1 replication for all the four cases. We can see the impressive performance of the proposed method. It also shows that the contrast between the two regions are visible for Cases G3 and G4, and the proposed method is capable to capture the boundary even though the distributions are misspecified.

TABLE 2

Performance of the methods for Gaussian noised images based on 100 simulations. The Lebesgue error between the estimated boundary the true boundary is presented. The maximum standard errors of each column are reported in the last row.

	Case G1	Case G2	Case G3	Case G4
Bayesian Method	0.00	0.01	0.01	0.01
CP5	0.03	0.63	0.62	0.61
CP31	0.02	0.64	0.63	0.62
SE	0.00	0.00	0.00	0.01

7. Proofs.

PROOF OF THEOREM 3.1. *Step 1: Prior concentration.* Let

$$B_n^*(\theta_0, \epsilon) = \left\{ \theta : \frac{1}{n} \sum_{i=1}^n K_i(\theta_0, \theta) \leq \epsilon^2, \frac{1}{n} \sum_{i=1}^n V_i(\theta_0, \theta) \leq \epsilon^2 \right\},$$

where $K_i(\theta_0, \theta) = K(P_{\theta_0, i}, P_{\theta, i})$ and $V_i(\theta_0, \theta) = V(P_{\theta_0, i}, P_{\theta, i})$. When $\|\xi - \xi_0\| \leq \epsilon^2$ and $\|\rho - \rho_0\| \leq \epsilon^2$ for some small ϵ , it follows that

$$\begin{aligned} K_i(\theta_0, \theta) &= K(\xi_0, \xi)P(X_i \in \Gamma_0 \cap \Gamma) + K(\rho_0, \rho)P(X_i \in \Gamma_0^c \cap \Gamma^c) \\ &\quad + K(\xi_0, \rho)P(X_i \in \Gamma_0 \cap \Gamma^c) + K(\rho_0, \xi)P(X_i \in \Gamma_0^c \cap \Gamma) \\ &\lesssim \|\xi_0 - \xi\|^2 + \|\rho_0 - \rho\|^2 + P(X_i \in \Gamma_0^c \cap \Gamma) + P(X_i \in \Gamma_0 \cap \Gamma^c) \\ (7.1) \quad &= \|\xi_0 - \xi\|^2 + \|\rho_0 - \rho\|^2 + n\lambda[(\Gamma_0 \Delta \Gamma) \cap T_i], \end{aligned}$$

according to the Assumption (A). Consequently, the average Kullback-Leibler divergence

$$\begin{aligned} (7.2) \quad \frac{1}{n} \sum_i K_i(\theta_0, \theta) &\lesssim \|\xi_0 - \xi\|^2 + \|\rho_0 - \rho\|^2 + \frac{1}{n} n\lambda[(\Gamma_0 \Delta \Gamma) \cap (\cup T_i)] \\ &= \|\xi_0 - \xi\|^2 + \|\rho_0 - \rho\|^2 + \lambda(\Gamma_0 \Delta \Gamma). \end{aligned}$$

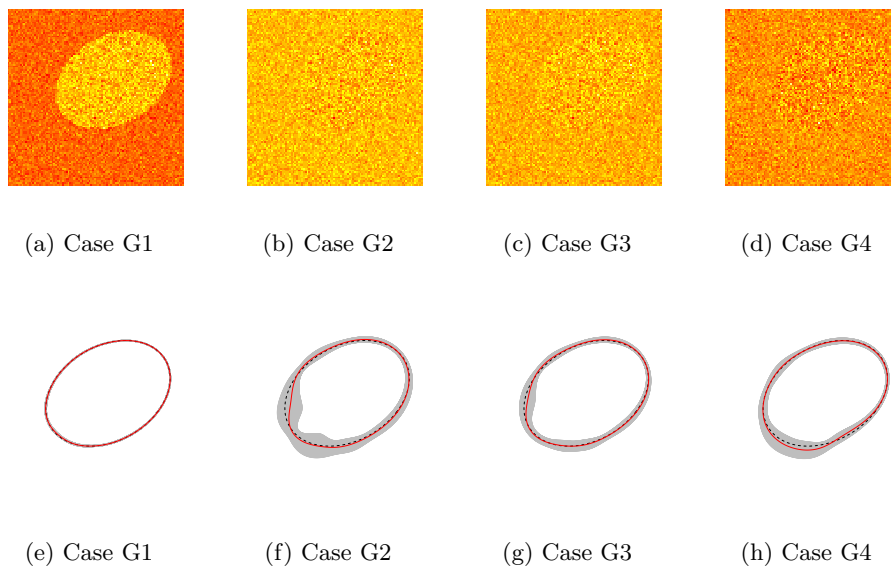


Fig 4: Proposed Bayesian estimates for Gaussian noised images with elliptic boundary. Plots (a)–(d) are the noisy observations. Figures (e)–(h) are the corresponding estimates (solid line in red) against the true boundary (dotted line in black), with a 95% uniform credible band (in gray).

Similarly, the second moment V_i of the log-likelihood ratio is also bounded in the same way, i.e. $V_i(\theta_0, \theta) \lesssim \|\xi_0 - \xi\|^2 + \|\rho_0 - \rho\|^2 + \lambda(\Gamma_0 \triangle \Gamma)$, which leads to

$$B_n^*(\theta_0, \epsilon) \supset \{(\xi, \rho, \gamma) : \|\xi_0 - \xi\|^2 \leq \epsilon^2/3, \|\rho_0 - \rho\|^2 \leq \epsilon^2/3, \lambda(\Gamma_0 \triangle \Gamma) \leq \epsilon^2/3\}.$$

By Assumption (B1), the prior density of (ξ, ρ) is bounded below in a neighborhood of (ξ_0, ρ_0) . Therefore, we have

$$\begin{aligned} \Pi(B_n^*(\theta_0, \epsilon)) &\gtrsim \Pi(\|\xi_0 - \xi\|^2 \leq \epsilon^2/3, \|\rho_0 - \rho\|^2 \leq \epsilon^2/3) \times \Pi(\lambda(\Gamma_0 \triangle \Gamma) \leq \epsilon^2/3) \\ &\gtrsim (1/\epsilon)^{2p} \times \Pi(\lambda(\Gamma_0 \triangle \Gamma) \leq \epsilon^2/3). \end{aligned}$$

Let ϵ_n be a sequence such that $\epsilon_n \rightarrow 0$ and $n\epsilon_n^2 \rightarrow \infty$. Then in order to ensure that $\Pi(B_n^*(\theta_0, \epsilon_n)) \geq \exp(-cn\epsilon_n^2)$ for some positive constant c , it is sufficient to have $\Pi(\lambda(\Gamma_0 \triangle \Gamma) \leq \epsilon_n^2) \gtrsim \exp(-cn\epsilon_n^2)$, or equivalently, $-\log \Pi(\gamma : \lambda(\Gamma_0 \triangle \Gamma) \leq \epsilon_n^2) \lesssim n\epsilon_n^2$ as in equation (3.1).

Step 2: Sieves. For each prior, we shall define a sieve Σ_n for γ , and thus use $\Theta_n = [-c_n, c_n]^p \times [-c_n, c_n]^p \times \Sigma_n$ as the sieve for θ . Noting that

$$\Pi(\Theta_n^c) \leq \Pi(\xi : \xi \notin [-c_n, c_n]^p) + \Pi(\rho : \rho \notin [-c_n, c_n]^p) + \Pi(\gamma : \gamma \notin \Sigma_n),$$

in order to ensure that the sieve covers most parameter space by $-\log \Pi(\Theta_n^c) \gtrsim n\epsilon_n^2$, it is sufficient to show $-\log \Pi(\Sigma_n^c) \gtrsim n\epsilon_n^2$ as in equation (3.2) if $-\log \Pi(\xi : \xi \notin [-c_n, c_n]^p) \gtrsim n\epsilon_n^2$ and $-\log \Pi(\rho : \rho \notin [-c_n, c_n]^p) \gtrsim n\epsilon_n^2$. For the later two conditions, we let $c_n = e^{n\epsilon_n^2}$, then $-\log \Pi(\xi : \xi \notin [-c_n, c_n]^p) \gtrsim -\log c_n^{-t_2}$ by Assumption (B2), which is $t_2 \cdot n\epsilon_n^2 \gtrsim n\epsilon_n^2$; similarly, we have $-\log \Pi(\rho : \rho \notin [-c_n, c_n]^p) \gtrsim n\epsilon_n^2$.

Step 3: Entropy bounds. Similarly to equation (7.2), the average of squared Hellinger distances d_n has the following bound when $\|\xi - \xi'\| \leq \epsilon$ and $\|\rho - \rho'\| \leq \epsilon$ for some small ϵ :

$$\begin{aligned} d_n^2(\theta, \theta') &= \frac{1}{n} \sum_{i=1}^n \int h^2(\phi_i, \phi'_i) dP_{X_i} \lesssim \|\xi - \xi'\|^2 + \|\rho - \rho'\|^2 + \lambda(\Gamma \triangle \Gamma') \\ &\lesssim \|\xi - \xi'\|^2 + \|\rho - \rho'\|^2 + \|\gamma - \gamma'\|_\infty \end{aligned}$$

by using Condition (A) and the relationship that the squared Hellinger distance is bounded by the Kullback-Leibler divergence. Therefore the entropy $\log N(\epsilon_n, \Theta_n, d_n)$ is bounded by

$$\begin{aligned} \log N(\epsilon_n^2, [-c_n, c_n]^p, \|\cdot\|) + \log N(\epsilon_n^2, [-c_n, c_n]^p, \|\cdot\|) + \log N(\epsilon_n^2, \Sigma_n, \|\cdot\|_\infty) \\ \lesssim \log \frac{2c_n}{\epsilon_n^2} + \log \frac{2c_n}{\epsilon_n^2} + \log N(\epsilon_n^2, \Sigma_n, \|\cdot\|_\infty). \end{aligned}$$

Recall that $c_n = e^{n\epsilon_n^2}$. Therefore $\log(2c_n/\epsilon_n^2) = \log 2 + \log(1/\epsilon_n^2) \lesssim n\epsilon_n^2$ given that $n\epsilon_n^2 \rightarrow \infty$ and $\log(1/\epsilon_n^2) \lesssim n\epsilon_n^2$. Hence, in order to ensure $\log N(\epsilon_n, \Theta_n, d_n) \lesssim n\epsilon_n^2$, it is sufficient to verify that $\log N(\epsilon_n^2, \Sigma_n, \|\cdot\|_\infty) \lesssim n\epsilon_n^2$ which is equation (3.3).

Then equation (3.4) follows by applying Theorem 4 of [15].

Equation (3.5) will follow if we can show that $d_n(\theta, \theta_0) \leq \epsilon_n$ implies that $\lambda(\Gamma \triangle \Gamma_0) \lesssim \epsilon_n^2$. As argued in the derivation of (7.2), $d_n^2(\theta, \theta')$ is given by

$$\begin{aligned} \frac{1}{n} \sum_i \int h^2(\phi, \phi') dP_{X_i} &= h^2(\xi_0, \xi) \lambda(\Gamma_0 \cap \Gamma) + h^2(\rho_0, \rho) \lambda(\Gamma_0^c \cap \Gamma^c) \\ &\quad + h^2(\xi_0, \rho) \lambda(\Gamma_0 \cap \Gamma^c) + h^2(\rho_0, \xi) \lambda(\Gamma_0^c \cap \Gamma). \end{aligned}$$

The above expression is larger than each of the following three expressions:

$$\begin{aligned}
& h^2(\xi_0, \xi)\lambda(\Gamma_0 \cap \Gamma) + h^2(\rho_0, \xi)\lambda(\Gamma_0^c \cap \Gamma) \\
& \geq \frac{(h(\xi_0, \xi) + h(\rho_0, \xi))^2}{2} \cdot (\lambda(\Gamma_0 \cap \Gamma) \wedge \lambda(\Gamma_0^c \cap \Gamma)), \\
& h^2(\rho_0, \rho)\lambda(\Gamma_0^c \cap \Gamma^c) + h^2(\xi_0, \rho)\lambda(\Gamma_0 \cap \Gamma^c) \\
& \geq \frac{(h(\rho_0, \rho) + h(\xi_0, \rho))^2}{2} \cdot (\lambda(\Gamma_0^c \cap \Gamma^c) \wedge \lambda(\Gamma_0 \cap \Gamma^c)), \\
& h^2(\xi_0, \rho)\lambda(\Gamma_0 \cap \Gamma^c) + h^2(\rho_0, \xi)\lambda(\Gamma_0^c \cap \Gamma) \\
& \geq \frac{(h(\xi_0, \rho) + h(\rho_0, \xi))^2}{2} \cdot (\lambda(\Gamma_0 \cap \Gamma^c) \wedge \lambda(\Gamma_0^c \cap \Gamma)).
\end{aligned}$$

We further have $h(\xi_0, \xi) + h(\rho_0, \xi) \geq h(\xi_0, \rho_0)$ and $h(\xi_0, \rho) + h(\rho_0, \rho) \geq h(\xi_0, \rho_0)$, by the triangle inequality, and $h(\xi_0, \rho) + h(\rho_0, \xi) \geq c_0 > 0$ by Condition (C). Combining with the last three displays respectively, we obtain

$$(7.3) \quad \lambda(\Gamma_0 \cap \Gamma) \wedge \lambda(\Gamma_0^c \cap \Gamma) \lesssim \epsilon_n^2$$

$$(7.4) \quad \lambda(\Gamma_0^c \cap \Gamma^c) \wedge \lambda(\Gamma_0 \cap \Gamma^c) \lesssim \epsilon_n^2$$

$$(7.5) \quad \lambda(\Gamma_0 \cap \Gamma^c) \wedge \lambda(\Gamma_0^c \cap \Gamma) \lesssim \epsilon_n^2,$$

whenever $d_n^2(\theta_0, \theta) \leq \epsilon_n^2$. By adding (7.3) and (7.4) to (7.5), we derive

$$(7.6) \quad \lambda(\Gamma_0) \wedge \lambda(\Gamma_0^c \cap \Gamma) \lesssim \epsilon_n^2, \quad \lambda(\Gamma_0^c) \wedge \lambda(\Gamma_0 \cap \Gamma^c) \lesssim \epsilon_n^2.$$

Since Γ_0 is fixed with $\lambda(\Gamma_0) > 0$ and $\lambda(\Gamma_0^c) > 0$ by the assumption, (7.6) implies that $\lambda(\Gamma_0^c \cap \Gamma) \lesssim \epsilon_n^2$, and $\lambda(\Gamma_0 \cap \Gamma^c) \lesssim \epsilon_n^2$. Consequently $\lambda(\Gamma_0 \triangle \Gamma) = \lambda(\Gamma_0^c \cap \Gamma) + \lambda(\Gamma_0 \cap \Gamma^c) \lesssim \epsilon_n^2$, which completes the proof. \square

PROOF OF LEMMA 3.2. For any $f'_{s'} \in \mathbb{H}'$, there is a series of α_i 's such that $f'_{s'}(\cdot) = \sum \alpha_i K(s', \cdot)$, and there exists $s \in [0, 1]^{d-1}$ such that $s' = Qs$. Let $f_s = \sum \alpha_i G(s, \cdot) \in \mathbb{H}$. Therefore, the map $\phi : \mathbb{H} \rightarrow \mathbb{H}'$, $\phi f_s = f'_{Qs}$ is surjective. If there exists another $s_2 \in [0, 1]^{d-1}$ such that $s' = Qs_2$ and $f_{s_2} = \sum \alpha_i G(s_2, \cdot) \in \mathbb{H}$, then $f_{s_2} = f_s$ because $f_s = \sum \alpha_i K(Qs, Q\cdot) = \sum \alpha_i K(Qs_2, Q\cdot) = f_{s_2}$. Therefore, the map ϕ is bijective. In addition, the definition of $G(\cdot, \cdot) : G(s_1, s_2) = K(Qs_1, Qs_2)$ also implies that the map ϕ is distance preserving when using $\|\cdot\|_{\mathbb{H}}$ and $\|\cdot\|_{\mathbb{H}'}$ as the norms. Therefore ϕ extends to an isometric isomorphism between \mathbb{H} and \mathbb{H}' . The map ϕ also preserves the distance if we use the $\|\cdot\|_{\infty}$ norm. \square

PROOF OF THEOREM 3.3. We verify equations (3.1),(3.2) and (3.3) in Theorem 3.1. Since $\|\gamma_0 - \beta_{0,J_n}^T \xi\|_\infty \leq \epsilon_n^2/2$, we have

$$\begin{aligned} & \Pi\{\gamma : \gamma = \beta^T \xi, \|\gamma - \gamma_0\|_\infty \leq \epsilon_n^2\} \\ & \geq \Pi(J = J_n)\Pi(\|\beta^T \xi - \beta_0^T \xi\|_\infty \leq \epsilon_n^2/2 | J = J_n) \\ & \geq \Pi(J = J_n)\Pi(\|\beta - \beta_0\|_1 \leq t_3^{-1} J^{-t_4} \epsilon_n^2/2 | J = J_n), \end{aligned}$$

where the last step is because $\|\beta_{1,J}^T \xi - \beta_{2,J}^T \xi\|_\infty \leq \|\beta_{1,J} - \beta_{2,J}\|_1 \max_{1 \leq j \leq J} \|\xi_j\|_\infty \leq t_3 J^{t_4} \|\beta_{1,J} - \beta_{2,J}\|_1$ according to the triangle inequality and Assumption (D). Therefore, we prove equation (3.1) by noting that $-\log \Pi\{\gamma : \gamma = \beta^T \xi, \|\gamma - \gamma_0\|_\infty \leq \epsilon_n^2\} \leq -\log \Pi(J = J_n) - \log \Pi(\|\beta - \beta_0\|_1 \leq t_3^{-1} J^{-t_4} \epsilon_n^2/2 | J = J_n) \lesssim J_n \log J_n + J_n \log(J_n/\epsilon_n) \lesssim J_n \log J_n + J_n \log n \lesssim n \epsilon_n^2$.

Considering the sieve $\Sigma_n = \{\gamma : \gamma = \beta^T \xi, \beta \in \mathbb{R}^j, j \leq J_n, \|\beta\|_\infty \leq \sqrt{n/C}\}$, the estimate of the prior mass of the complement of the sieve is given by $\Pi(\gamma : \gamma \notin \Sigma_n) \leq \Pi(J > J_n) + J_n e^{-n}$ (see equation (2.10) in [39]). For any $a, b > 0$, we have $\log(a+b) \leq \log(2(a \vee b))$, therefore $-\log(a+b) \geq -\log 2 + (-\log a) \wedge (-\log b)$. Noting that $-\log \Pi(J > J_n) \gtrsim J_n \log J_n$, and $-\log(J_n e^{-n}) = n - \log J_n \gtrsim J_n \log J_n$, we then obtain $-\log \Pi(\gamma : \gamma \notin \Sigma_n) \gtrsim J_n \log J_n \gtrsim n \epsilon_n^2$ verifying equation (3.2).

For the entropy calculation, we first estimate the packing number $D(\epsilon_n^2, \Sigma_n, \|\cdot\|_\infty)$ by

$$\sum_{j=1}^{J_n} D(\epsilon_n^2, \{\beta \in \mathbb{R}^j, \|\beta\|_\infty \leq \sqrt{n/C}\}, \|\cdot\|_\infty) \leq \sum_{j=1}^{J_n} \left(1 + \frac{\sqrt{n/C}}{\epsilon_n}\right)^j,$$

which is further bounded by $J_n(1 + \sqrt{n/C}/\epsilon_n^2)^{J_n}$. Equation (3.3) follows since $\log N(\epsilon_n^2, \Sigma_n, \|\cdot\|_\infty) \leq \log D(\epsilon_n^2, \Sigma_n, \|\cdot\|_\infty) \lesssim \log J_n + J_n \log n + J_n \log_- \epsilon_n^2 \lesssim J_n \log n \lesssim n \epsilon_n^2$. \square

PROOF OF LEMMA 4.1. The generating function of $I_n(2x)$ is given in Proposition 8.1 (a): $e^{x(z+1/z)} = \sum_{n=-\infty}^{\infty} I_n(2x) z^n$ for $z \in \mathbb{C}$ and $z \neq 0$. Let $x = a^2$ and $z = e^{-2\pi i t}$, noting that $z + 1/z - 2 = -4 \sin^2(\pi t)$, we then have $\phi_a(t) = \exp\{-4a^2 \sin^2(\pi t)\} = \sum_{n=-\infty}^{\infty} e^{-2a^2} I_n(2a^2) e^{-2n\pi i t}$. By defining μ_a as the discrete measure in Lemma 4.1, we obtain that $\phi_a(t) = \int e^{-its} d\mu_a(s)$.

Furthermore, $G_a(t, t') = \phi_a(t - t') = \sum_{n=-\infty}^{\infty} e^{-2a^2} I_n(2a^2) e^{-2n\pi i(t-t')}$. In view of the orthonormality of $\{e^{2n\pi i} : n \in \mathbb{Z}\}$, we obtain that the integral $\int_0^1 K(t, t') e^{2\pi n i t} dt = e^{-2a^2} I_n(2a^2) e^{2\pi n i t'}$ for any $n \in \mathbb{Z}$. Hence the trigonometric polynomials $\{1, \cos 2n\pi t, \sin 2n\pi t : n \geq 1\}$ form the eigenfunction

basis of the covariance kernel $G_a(\cdot, \cdot)$, where the corresponding eigenvalues are $\{e^{-2a^2} I_n(2a^2), e^{-2a^2} I_n(2a^2) : n \geq 0\}$. \square

PROOF OF LEMMA 4.2. Since the measure μ_a has subexponential tail, Lemma 2.1 in [41] is directly applicable. Using the discrete measure μ_a defined in Lemma 4.1, the proof follows. \square

PROOF OF LEMMA 4.3. By Jackson's theorem [19], for any function $w \in \mathbb{C}^\alpha[0, 1]$, we have $\|w - h_N\|_\infty \leq A_w N^{-\alpha}$ for some $h_N = \sum_{n=-N}^N a_n e^{-i2\pi n}$, where A_w is a constant depending only on w . Clearly this $h_N \in \mathbb{H}^a$ and by Lemma 4.2 its square norm is

$$\|h_N\|_{\mathbb{H}^a}^2 = \sum_{n=-N}^N \frac{1}{e^{-2a^2} I_n(2a^2)} \left| \int_0^1 h_N(t) e^{it2\pi n} dt \right|^2.$$

Using the monotonicity of $I_n(2a^2)$ for fixed a (Proposition 8.1 (b) and (c2)), we have $e^{-2a^2} I_n(2a^2) \geq e^{-2a^2} I_N(2a^2)$ for $n = 0, \pm 1, \dots, \pm N$. Therefore,

$$\|h_N\|_{\mathbb{H}^a}^2 \leq \frac{1}{e^{-2a^2} I_N(2a^2)} \sum_{n=-N}^N \left| \int_0^1 h_N(t) e^{it2\pi n} dt \right|^2 \leq \frac{1}{e^{-2a^2} I_N(2a^2)} \|h_N\|_2^2.$$

Let $N \asymp a$, then $N^{-\alpha} \asymp a^{-\alpha}$, and $e^{-2a^2} I_N(2a^2) \asymp a^{-1}$ according to Proposition 8.2. On the other hand, $\|h_N\|_2^2 \rightarrow \|w\|_2^2$ which is finite. Therefore, it follows that $\|h_N\|_{\mathbb{H}^a}^2 \leq D_w a$ for a constant D_w depending only on w . \square

PROOF OF LEMMA 4.4. We construct an ϵ -net of piecewise polynomials over \mathbb{H}_1^a similarly to the one used in the proof of Lemma 2.3 in [41]. Let β_{2k}^a to be the $2k$ th absolute moments of the spectral measure μ_a , i.e. $\beta_{2k}^a = \sum_{n=-\infty}^{\infty} e^{-2a^2} I_n(2a^2) (2\pi|n|)^{2j}$. In the case of [41], $\beta_{2k}^a = \beta_{2k}^1 / a^{2k}$, but here we do not have this simple relationship and need to work with β_{2k}^a directly. Following the same construction in [41] but use β_{2k}^a , we can obtain that

$$\log N(2\epsilon, \mathbb{H}_1^a, \|\cdot\|_\infty) \leq \left(\frac{1}{\delta} + 1 \right) \sum_{j=0}^{k-1} \log \left(2\sqrt{\beta_{2j}^a} \frac{\delta^j}{j!} \cdot \frac{k}{\epsilon} + 1 \right),$$

where $k \in \mathbb{N}$ such that $\sqrt{\beta_{2k}^a} d^k / k! \leq \epsilon$ for given $\epsilon, \delta > 0$.

For any $a \geq 0$ and $j \geq 0$, applying Proposition 8.3 with $x = a^2$, we get

$$\beta_{2j}^a = (2\pi)^{2j} \sum_{n=-\infty}^{\infty} e^{-2a^2} I_n(2a^2) n^{2j} \leq (2\pi)^{2j} \frac{(4j)!}{(2j)!} \max(a^{2j}, 1).$$

Choose $\delta = 1/\{16\pi \max(a, 1)\}$, then $\sqrt{\beta_{2j}^a} \delta^j / j! \leq 8^{-j} \sqrt{(4j)! / (2j)!} / (j!)$. Using Stirling's approximation with explicit bounds: $\sqrt{2\pi} n^{n+1/2} e^{-n} \leq n! \leq e n^{n+1/2} e^{-n}$ for all positive integers n , for $j \geq 1$, we obtain

$$\sqrt{\beta_{2j}^a} \frac{\delta^j}{j!} \leq \frac{\sqrt{e} (4j)^{2j+1/4} e^{-2j}}{(2\pi)^{3/4} (2j)^{j+1/4} e^{-j} j^{j+1/2} e^{-j} \cdot 8^j} \leq \sqrt{e} (2\pi)^{-3/4} 2^{1/4}.$$

When $j = 0$, $\sqrt{\beta_{2j}^a} \delta^j / j! \leq 1$. Therefore, we have a uniform bound for $\sqrt{\beta_{2j}^a} \delta^j / j!, j \geq 0$. Let $k \sim \log(1/\epsilon)$, we then have $\log N(2\epsilon, \mathbb{H}_1^a, \|\cdot\|_\infty) \lesssim (1/\delta + 1)k \log(k/\epsilon) \lesssim \max(a, 1)\{\log(1/\epsilon)\}^2$, concluding the proof. \square

PROOF OF LEMMA 4.5. In view of Lemma 4.4, the proof follows the argument in Lemma 4.6 in [43] by letting $d = 2$. \square

PROOF OF LEMMA 4.7. We need to show that if $a \leq b$ and $f \in \sqrt{a}\mathbb{H}_1^a$, i.e., $\|f\|_{\mathbb{H}^a}^2 \leq \sqrt{a}$, then $\|f\|_{\mathbb{H}^b}^2 \leq \sqrt{cb}$. By Lemma 4.2, it is sufficient to show that $ae^{-2a^2} I_n(2a^2) \leq cbe^{-2b^2} I_n(2b^2)$ for any $n \geq 0$. Let the function $f_n(x) = \sqrt{x}e^{-x} I_n(x)$, then we just need to show that $f_n(\sqrt{2a})/f_n(\sqrt{2b}) \leq c$. By Proposition 8.4, we have $f_n(\sqrt{2a})/f_n(\sqrt{2b}) \leq 1$ for $n \geq 2$.

When $n = 0$, Proposition 8.4 indicates that $f_0(x)$ is increasing in x for $x \leq 1/2$, and Proposition 8.2 implies that there exists constants $c_1, c_2 > 0$ such that $f_0(x) \in (c_1, c_2)$ for $x \in [1/2, \infty)$. Therefore, if $b \leq 1/8$, we have $f_0(\sqrt{2a}) \leq f_0(\sqrt{2b})$. If $b > 1/8$, we then have $f_0(\sqrt{2a})/f_0(\sqrt{2b}) \leq \max\{f_0(1/2), c_2\}/c_1 < \infty$. Consequently, for $a \leq b$, we have $f_0(\sqrt{2a}) \leq \max\{f_0(1/2)/c_1, c_2/c_1, 1\}f_0(\sqrt{2b})$. Similarly when $n = 1$, the function $f_1(x)$ is increasing in x for $x \leq 3/2$ and there exists two constants $c_3, c_4 > 0$ such that $f_1(x) \in (c_3, c_4)$ for $x \in [3/2, \infty)$. Consequently, we have $f_1(\sqrt{2a}) \leq \max\{f_1(3/2)/c_3, c_4/c_3, 1\}f_1(\sqrt{2b})$. We conclude the proof by letting $c = \max\{f_0(1/2)/c_1, c_2/c_1, f_1(3/2)/c_3, c_4/c_3, 1\}$. \square

PROOF OF LEMMA 4.8. By Lemma 4.2, an element in \mathbb{H}_a^a can be viewed as the real part of $h(t) = \sum_{n=-\infty}^{\infty} e^{-it2\pi n} b_{n,a} e^{-2a^2} I_n(2a^2)$, where $b_{n,a}$ satisfies that $\sum_{n=-\infty}^{\infty} |b_{n,a}|^2 e^{-2a^2} I_n(2a^2) \leq 1$. Applying the Cauchy-Schwartz inequality twice, we have $|h(0)|^2 \leq \sum_{n=-\infty}^{\infty} e^{-2a^2} I_n(2a^2) = 1$ and $|h(t) - h(0)|^2 \leq t^2 \sum_{n=-\infty}^{\infty} (2\pi n)^2 e^{-2a^2} I_n(2a^2)$. By Proposition 8.5, we have $|h(t) - h(0)|^2 \leq 8\pi^2 a^2 t^2$. This concludes the proof. \square

PROOF OF THEOREM 4.6. The established properties of the RKHS of W^a from Lemma 4.2 to Lemma 4.8 are parallel to the case when a GP

is indexed by $[0, 1]^{d-1}$ with a stationary kernel, therefore, we can directly follow the argument in the proof of Theorem 3.1 in [43]. There is a small modification since the nesting property given in Lemma 4.7 has a universal constant c , which is straightforward and does not affect the asymptotic rate. The posterior contraction rate ϵ_n^2 is thus obtained, which is the same as deterministic rescaling in Section 4.2 up to a logarithmic factor but adaptive to the unknown smoothness level α . \square

8. Modified Bessel function of the first kind. The modified Bessel function of the first kind are solutions to the modified Bessel's equation [45]. Throughout the paper, we consider integer orders and positive argument, i.e. $I_n(x)$ with $n \in \mathbb{Z}$ and $x > 0$. We first introduce some basic properties of $I_n(x)$ in Proposition 8.1, for easy reference.

PROPOSITION 8.1. *The modified Bessel functions $I_n(2x)$ has the following properties:*

(a) *Generating functions. For $x \in \mathbb{R}$,*

$$G(x, z) =: e^{x(z+1/z)} = \sum_{n=-\infty}^{\infty} I_n(2x)z^n, \quad z \in \mathbb{C}, z \neq 0.$$

(b) *Symmetry about the order: $I_n(2x) = I_{-n}(2x)$ for $x \in \mathbb{R}$ and $n \in \mathbb{Z}$.*

(c) *For $n \geq 0$ and fixed $x > 0$, the following properties hold.*

(c1) *Series representation: $I_n(2x) = x^n \sum_{j=0}^{\infty} x^{2j} / (j!(n+j)!)$.*

(c2) *$I_n(2x)$ is positive and strictly decreasing in n .*

(c3) *$I_n(2x) \leq I_0(2x)x^n/n!$, i.e., $I_n(2x)$ decays like a factorial as n increases.*

PROOF. Properties (a), (b) and (c1) can be found in most literature on Bessel functions, e.g., see Chapter II of [45] and 8.51–8.52 of [20]. The positiveness of $I_n(2x)$ follows its series representation. For (c2) and (c3), we let $r_n(x) = I_{n+1}(2x)/I_n(2x)$ where $n \geq 0$ and $x > 0$. Then by [1], we have

$$(8.1) \quad r_n(x) \leq \frac{2x}{n + 1/2 + (4x^2 + (n + 1/2)^2)^{1/2}} < 1,$$

leading to the monotonicity in (c2). Equation (8.1) also implies that $r_n(x) \leq x/n$ for all $n \geq 0$, and hence $I_{n+1}(2x) \leq I_0(2x)x^n/n!$, concluding (c3). \square

PROPOSITION 8.2. *Let $n \in \mathbb{Z}^+$ and $nx^{-1/2} \rightarrow c$ for some constant $c \geq 0$, then $e^{-x}I_n(x) \asymp x^{-1/2}$ as $n, x \rightarrow \infty$.*

PROOF. The integral formula for the modified Bessel function of the first kind [45, page 181] implies that, for $n \in \mathbb{Z}^+$, $I_n(x)$ is

$$\frac{1}{\pi} \int_0^\pi e^{x \cos t} \cos(nt) dt = \frac{1}{\pi} \int_0^{\pi/2} e^{x \cos t} \cos(nt) dt + \frac{1}{\pi} \int_{\pi/2}^\pi e^{x \cos t} \cos(nt) dt.$$

The second integral is bounded since $\cos t \leq 0$ for $t \in [\pi/2, \pi]$. For the first integral, we set $u = 2\sqrt{x} \sin(t/2)$, then we have

$$I_n(x) = \frac{e^x}{\pi\sqrt{x}} \int_0^{2\sqrt{x}} e^{-\frac{u^2}{2}} \cos\left(2n \arcsin\left(\frac{u}{2\sqrt{x}}\right)\right) \left(1 - \frac{u^2}{4x}\right) du + O(1).$$

View x as a function of n , i.e., $x = x_n$, and denote the integrand by

$$f_n(u) = e^{-\frac{u^2}{2}} \cos\left(2n \arcsin\left(\frac{u}{2\sqrt{x}}\right)\right) \left(1 - \frac{u^2}{4x}\right) \mathbb{1}(0 < u < 2\sqrt{x}).$$

If $nx^{-1/2} \rightarrow c$ for a constant $c \geq 0$, we have $f_n(u) \rightarrow e^{-\frac{u^2}{2}} \cos(cu)$. Therefore,

$$e^{-x} I_n(x) \sqrt{x} \rightarrow \pi^{-1} \int_0^\infty e^{-\frac{u^2}{2}} \cos(cu) du = (2\pi)^{-1/2} e^{-\frac{c^2}{2}},$$

where the last step uses the real part of the characteristic function of a standard normal. □

PROPOSITION 8.3. *For any $x \geq 0$ and $j = 0, 1, 2, \dots$, we have*

$$\sum_{n=-\infty}^{\infty} e^{-2x} I_n(2x) n^{2j} \leq \frac{(4j)!}{(2j)!} \max(x^j, 1).$$

PROOF. Let $G_j(x, z) = z^{2j} e^{x(z+1/z)}$, then by Proposition 8.1 (a), we have $G_j(x, z) = \sum_{n=-\infty}^{\infty} I_n(2x) z^{n+2j}$. When $j = 0$, we thus have $\sum_{n=-\infty}^{\infty} e^{-2x} I_n(2x) n^{2j} = 1$, leading to the statement of the proposition. For $j \geq 1$, we first take the $2j$ th partial derivatives of $G_{2j}(x, z)$ and obtain

$$\frac{\partial^{2j} G_j(x, z)}{\partial z^{2j}} = \sum_{n=-\infty}^{\infty} I_n(2x) (n+2j)_{2j} z^n,$$

where $(n+2j)_{2j} = (n+2j) \cdot (n+2j-1) \cdots (n+1)$ is the falling factorial. It is easy to see that for $n \geq 0$, $(n+2j)_{2j} \geq n^{2j}$; for $n \in [-2j, -1]$, $(n+2j)_{2j} = 0$;

for $n < -2j$, $(n+2j)_{2j} = (-1)^{2j}(-n-2j) \cdots (-n-1) \geq 0$. Therefore, we have for $z > 0$,

$$(8.2) \quad \frac{\partial^{2j} G_j(x, z)}{\partial z^{2j}} \geq \sum_{n=0}^{\infty} I_n(2x) n^{2j} z^n = \sum_{n=1}^{\infty} I_n(2x) n^{2j} z^n.$$

Let $F_j(x) = \left. \frac{\partial^{2j} G_j(x, z)}{\partial z^{2j}} \right|_{z=1}$, then equation (8.2) implies that

$$(8.3) \quad \sum_{n=-\infty}^{\infty} e^{-2x} I_n(2x) n^{2j} = 2 \sum_{n=1}^{\infty} e^{-2x} I_n(2x) n^{2j} \leq 2e^{-2x} F_j(x).$$

To bound $F_j(x)$, consider $H_j(x, z) = \log\{G_j(x, z)\} = 2j \log z + x(z + z^{-1})$. By direct calculation, the p th order derivative of $H_j(x, z)$ is given by

$$\frac{\partial^p H_j(x, z)}{\partial z^p} = \begin{cases} 2jz^{-1} + x - xz^{-2}, & \text{if } p = 1, \\ (-1)^p p! (-2jp^{-1}z + x) z^{-(p+1)}, & \text{if } p \geq 2. \end{cases}$$

Applying the Faà di Bruno's formula, we have

$$(8.4) \quad \frac{\partial^{2j} G_j(x, z)}{\partial z^{2j}} = \sum_{\mathcal{K}} \frac{(2j)!}{k_1! \cdots k_{2j}!} e^{H_j(x, z)} \cdot \prod_{i=1}^{2j} \left\{ \frac{\partial^i H_j(x, z)}{\partial z^i} \cdot \frac{1}{i!} \right\}^{k_i},$$

where the sum is over the set $\mathcal{K} = \{(k_1, \dots, k_{2j}) : \sum_{i=1}^{2j} ik_i = 2j, k_i \in \{0\} \cup \mathbb{Z}^+\}$. Plugging in the expression of $\partial^p H_j(x, z)/\partial z^p$ and $z = 1$, equation (8.4) leads to

$$\begin{aligned} F_j(x) &= \left. \frac{\partial^{2j} G_j(x, z)}{\partial z^{2j}} \right|_{z=1} = \sum_{\mathcal{K}} \frac{(2j)!}{k_1! \cdots k_{2j}!} e^{2x} \prod_{i=2}^{2j} \left\{ (-1)^i \left(-\frac{2j}{i} + x \right) \right\}^{k_i} (2j)^{k_1} \\ &= \sum_{\mathcal{K}} \frac{(2j)!}{k_1! \cdots k_{2j}!} e^{2x} (-1)^{\sum_{i=1}^{2j} ik_i} \prod_{i=2}^{2j} \left\{ \left(-\frac{2j}{i} + x \right) \right\}^{k_i} (-2j)^{k_1} \\ &= \sum_{\mathcal{K}} \frac{(2j)!}{k_1! \cdots k_{2j}!} e^{2x} \prod_{i=2}^{2j} \left\{ \left(-\frac{2j}{i} + x \right) \right\}^{k_i} (-2j)^{k_1}, \end{aligned}$$

where the last step is because $\sum_{i=1}^{2j} ik_i = 2j$ which is even.

Noting that $2j/i \geq 1$ for $i = 2, \dots, 2j$, it is easy to verify that $|-2j/i + x| \leq \max(x, 1)2j/i$ for $x \geq 0$. Consequently, we have

$$(8.5) \quad \begin{aligned} |F_j(x)| &\leq \sum_{\mathcal{K}} \frac{(2j)!}{k_1! \cdots k_{2j}!} e^{2x} \prod_{i=2}^{2j} \{\max(x, 1)\}^{k_i} \left\{ \left(\frac{2j}{i} \right) \right\}^{k_i} (2j)^{k_1} \\ &\leq \sum_{\mathcal{K}} \frac{(2j)!}{k_1! \cdots k_{2j}!} e^{2x} \{\max(x, 1)\}^{\sum_{i=2}^{2j} k_i} \prod_{i=1}^{2j} \left(\frac{2j}{i} \right)^{k_i}. \end{aligned}$$

Furthermore, for $(k_1, \dots, k_{2j}) \in \mathcal{K}$, we have $\sum_{i=2}^{2j} k_i \leq \sum_{i=2}^{2j} ik_i = 2j - k_1 \leq 2j$, thus $\sum_{i=2}^{2j} k_i \leq j$. Consequently, equation (8.5) leads to

$$|F_j(x)| \leq e^{2x} \max(x^j, 1) \sum_{\mathcal{K}} \frac{(2j)!}{k_1! \cdots k_{2j}!} \prod_{i=1}^{2j} \left(\frac{2j}{i}\right)^{k_i} =: e^{2x} \max(x^j, 1) A_{2j}.$$

To estimate A_{2j} , let $\mathcal{K}_k = \mathcal{K} \cap \{(k_1, \dots, k_{2j}) : \sum_{i=1}^{2j} k_i = k\}$, we then have $A_{2j} = \sum_{k=1}^{2j} (2j)^k \sum_{\mathcal{K}_k} (2j)! / (k_1! \cdots k_{2j}!) \prod_{i=1}^{2j} (1/i)^{k_i} = \sum_{k=1}^{2j} (2j)^k B_{2j,k}(0!, 1!, \dots)$, where $B_{2j,k}(0!, 1!, \dots)$ is the so-called Bell polynomials evaluated at $(0!, 1!, \dots)$ and is equal to the unsigned Stirling number of the first kind $|s(2j, k)|$ [Theorems A and B, page 133–134 in 7]. Therefore, we have $A_{2j} = \sum_{k=1}^{2j} |s(2j, k)| (2j)^k$, which is equal to $(2j)(2j+1) \cdots (2j+2j-1) = (4j)! / \{2(2j)!\}$ according to the generating function of $|s(2j, k)|$ [equation (5f), page 213 in 7]. Therefore, $|F_j(x)| \leq e^{2x} \max(x^j, 1) (4j)! / \{2(2j)!\}$. Combining equation (8.3), this yields the bound given in the statement of the proposition. \square

PROPOSITION 8.4. *The function $f_n(x) = \sqrt{x}e^{-x}I_n(x)$ is increasing in x when $x \in B_n$, where $B_n = [0, n + 1/2]$ if $n = 0, 1$ and $B_n = [0, \infty)$ if $n \geq 2$.*

PROOF. For given $n \geq 0$, let $g_n(x) = \log f_n(x) = (\log x)/2 - x + \log I_n(x)$. Then $g'_n(x) = 1/(2x) - 1 + I'_n(x)/I_n(x)$. Let $r_n(x) = I_{n+1}(x)/I_n(x)$, then $I'_n(x)/I_n(x) = r_n(x) + n/x$ (equation (8) in [1]). Therefore, the increasing property of $f_n(x)$ follows if we show that $1/(2x) - 1 + r_n(x) + n/x \geq 0$, or equivalently $r_n(x) \geq 1 - (n + 1/2)/x$.

Since $r_n(x) \geq 0$ for $n \geq 0$ and $x \geq 0$, $f_n(x)$ is thus increasing in $x \in [0, n + 1/2]$ for any $n \geq 0$. When $n \geq 2$, we shall use the lower bound for $r_n(x)$ given in [1], i.e. $r_n(x) \geq x(n + 1/2 + \{x^2 + (n + 3/2)^2\}^{1/2})$ when $x \geq 0$. Let $t = n + 1/2$, then it is sufficient to show that $x(n + 1/2 + \{x^2 + (n + 3/2)^2\}^{1/2}) \geq 1 - t/x$ for $x > t \geq 5/2$. We rewrite this inequality as $x^2 - (x - t)t \geq (x - t)\sqrt{x^2 + (t + 1)^2}$, which is simplified as $x^2 t^2 \geq (x - t)^2(2t + 1)$ by algebra. It follows the observation that when $x > t \geq 5/2$, we have $x > x - t > 0$ and $t^2 > 2t + 1$. Therefore, $f_n(x)$ is increasing in x if $n \geq 2$. \square

PROPOSITION 8.5. *For any $x \geq 0$, we have $\sum_{n=-\infty}^{\infty} e^{-2x} I_n(2x) n^2 = 2x$.*

PROOF. Let $G_2(x, z) = z^2 e^{x(z+1/z)}$, then a direct calculation leads to that $\partial G_2(x, z) / \partial z = e^{x(z+z^{-1})} (xz^2 - x + 2z)$ and $\partial^2 G_2(x, z) / \partial z^2 = e^{x(z+z^{-1})} \{(x - xz^{-2})(xz^2 - x + 2z) + 2xz + 2\}$. On the other hand, by Proposition 8.1 (a),

we have $G_2(x, z) = \sum_{n=-\infty}^{\infty} I_n(2x)z^{n+2}$. We take derivatives at the right hand side term by term and obtain that

$$\sum_{n=-\infty}^{\infty} e^{-2x} I_n(2x)n^2 = \frac{\partial^2 G_2(x, 1)}{\partial z^2} - 3 \frac{\partial G_2(x, 1)}{\partial z} + 4G_2(x, 1),$$

which is $2x$ by plugging the expression of $\partial G_2(x, z)/\partial z$, $\partial^2 G_2(x, z)/\partial z^2$ and letting $z = 1$. \square

ACKNOWLEDGEMENTS

We thank Professor Aad van der Vaart for many helpful discussions and pointing out important references. The work was conducted when the first author was a graduate student at North Carolina State University.

REFERENCES

- [1] AMOS, D. (1974). Computation of modified Bessel functions and their ratios. *Mathematics of Computation* **28** 239–251.
- [2] BANERJEE, S. and GELFAND, A. E. (2006). Bayesian Wombling: Curvilinear Gradient Assessment Under Spatial Process Models. *Journal of the American Statistical Association* **101** 1487–1501.
- [3] BASU, M. (2002). Gaussian-based edge-detection methods—a survey. *IEEE Transactions on Systems, Man, and Cybernetics, Part C* **32** 252–260.
- [4] BHARDWAJ, S. and MITTAL, A. (2012). A Survey on Various Edge Detector Techniques. *Procedia Technology* **4** 220–226.
- [5] CARLSTEIN, E. and KRISHNAMOORTHY, C. (1992). Boundary estimation. *Journal of the American Statistical Association* **87** 430–438.
- [6] CHEN, J. and GUPTA, A. K. (2011). *Parametric Statistical Change Point Analysis: With Applications to Genetics, Medicine, and Finance*. Springer Science & Business Media.
- [7] COMTET, L. (1974). *Advanced Combinatorics: The Art of Finite and Infinite Expansions*. D. Reidel Publishing Company, Dordrecht, Holland.
- [8] DAI, F. and XU, Y. (2013). *Approximation Theory and Harmonic Analysis on Spheres and Balls*. Springer.
- [9] DONOHO, D. L. (1999). Wedgelets: Nearly minimax estimation of edges. *The Annals of Statistics* **27** 859–897.
- [10] DUDLEY, R. M. (1974). Metric entropy of some classes of sets with differentiable boundaries. *Journal of Approximation Theory* **10** 227–236.
- [11] ENNIS, D. (2005). Spherical Harmonics. <http://www.mathworks.com/matlabcentral/fileexchange/8638-spherical-harmonics>. MATLAB Central File Exchange.
- [12] FITZPATRICK, M. C., PREISSER, E. L., PORTER, A., ELKINTON, J., WALLER, L. A., CARLIN, B. P. and ELLISON, A. M. (2010). Ecological boundary detection using Bayesian areal wombling. *Ecology* **91** 3448–3455.
- [13] GEMAN, S. and GEMAN, D. (1984). Stochastic relaxation, Gibbs distributions, and the Bayesian restoration of images. *Pattern Analysis and Machine Intelligence, IEEE Transactions on* **6** 721–741.

- [14] GEMAN, S. and GEMAN, D. (1993). Stochastic relaxation, Gibbs distributions and the Bayesian restoration of images. *Journal of Applied Statistics* **20** 25-62.
- [15] GHOSAL, S. and VAN DER VAART, A. (2007). Convergence rates of posterior distributions for noniid observations. *The Annals of Statistics* **35** 192-223.
- [16] GU, K., PATI, D. and DUNSON, D. B. (2014). Bayesian Multiscale Modeling of Closed Curves in Point Clouds. *Journal of the American Statistical Association* **109** 1481-1494.
- [17] HALL, P., PENG, L. and RAU, C. (2001). Local likelihood tracking of fault lines and boundaries. *Journal of the Royal Statistical Society: Series B (Statistical Methodology)* **63** 569-582.
- [18] HASTIE, T. and STUETZLE, W. (1989). Principal curves. *Journal of the American Statistical Association* **84** 502-516.
- [19] JACKSON, D. (1930). *The Theory of Approximation* **11**. The American Mathematical Society.
- [20] JEFFREY, A. and ZWILLINGER, D. (2007). *Table of Integrals, Series, and Products. Table of Integrals, Series, and Products Series*. Elsevier Science.
- [21] KILLICK, R. and ECKLEY, I. A. (2011). Changepoint: an R package for change-point analysis. *R package version 0.6*, URL <http://CRAN.R-project.org/package=changepoint>.
- [22] KILLICK, R., FEARNHEAD, P. and ECKLEY, I. (2012). Optimal detection of change-points with a linear computational cost. *Journal of the American Statistical Association* **107** 1590-1598.
- [23] KOROSTELEV, A. P. and TSYBAKOV, A. B. (1993). *Minimax Theory of Image Reconstruction. Lecture Notes in Statistics, 82*. Springer, New York.
- [24] KUELBS, J. and LI, W. V. (1993). Metric entropy and the small ball problem for Gaussian measures. *Journal of Functional Analysis* **116** 133-157.
- [25] LI, W. V. and LINDE, W. (1999). Approximation, metric entropy and small ball estimates for Gaussian measures. *The Annals of Probability* **27** 1556-1578.
- [26] LU, H. and CARLIN, B. P. (2005). Bayesian Areal Wombling for Geographical Boundary Analysis. *Geographical Analysis* **37** 265-285.
- [27] MACKAY, D. J. (1998). Introduction to Gaussian processes. *NATO ASI Series F Computer and Systems Sciences* **168** 133-166.
- [28] MAMMEN, E. and TSYBAKOV, A. (1995). Asymptotical minimax recovery of sets with smooth boundaries. *The Annals of Statistics* **23** 502-524.
- [29] MÜLLER, H.-G. and SONG, K.-S. (1994). Maximin estimation of multidimensional boundaries. *Journal of Multivariate Analysis* **50** 265-281.
- [30] NEAL, R. M. (2003). Slice sampling. *The Annals of Statistics* **31** 705-767.
- [31] POLZEHL, J. and SPOKOINY, V. (2003). Image denoising: pointwise adaptive approach. *The Annals of Statistics* **31** 30-57.
- [32] QIU, P. (2005). *Image Processing and Jump Regression Analysis* **599**. John Wiley & Sons.
- [33] QIU, P. (2007). Jump surface estimation, edge detection, and image restoration. *Journal of the American Statistical Association* **102** 745-756.
- [34] QIU, P. and SUN, J. (2007). Local smoothing image segmentation for spotted microarray images. *Journal of the American Statistical Association* **102** 1129-1144.
- [35] QIU, P. and SUN, J. (2009). Using conventional edge detectors and postsMOOTHING for segmentation of spotted microarray images. *Journal of Computational and Graphical Statistics* **18** 147-164.
- [36] QIU, P. and YANDELL, B. (1997). Jump detection in regression surfaces. *Journal of Computational and Graphical Statistics* **6** 332-354.

- [37] RASMUSSEN, C. E. and WILLIAMS, C. K. (2006). *Gaussian Process for Machine Learning. Adaptive Computation and Machine Learning.* the MIT Press.
- [38] RUDEMO, M. and STRYHN, H. (1994). Approximating the Distribution of Maximum Likelihood Contour Estimators in Two-Region Images. *Scandinavian Journal of Statistics* **21** 41–55.
- [39] SHEN, W. and GHOSAL, S. (2014). Adaptive Bayesian procedures using random series prior. *arXiv preprint arXiv:1403.0625*. To appear in Scandinavian Journal of Statistics.
- [40] TERRAS, A. (2013). *Harmonic Analysis on Symmetric Spaces—Euclidean Space, the Sphere, and the Poincaré Upper Half-Plane.* Springer.
- [41] VAN DER VAART, A. and VAN ZANTEN, H. (2007). Bayesian inference with rescaled Gaussian process priors. *Electronic Journal of Statistics* **1** 433–448.
- [42] VAN DER VAART, A. W. and VAN ZANTEN, J. H. (2008). Rates of contraction of posterior distributions based on Gaussian process priors. *The Annals of Statistics* **36** 1435–1463.
- [43] VAN DER VAART, A. W. and VAN ZANTEN, J. H. (2009). Adaptive Bayesian estimation using a Gaussian random field with inverse Gamma bandwidth. *The Annals of Statistics* **37** 2655–2675.
- [44] WALLER, L. A. and GOTWAY, C. A. (2004). *Applied Spatial Statistics for Public Health Data* **368**. John Wiley & Sons.
- [45] WATSON, G. N. (1995). *A Treatise on the Theory of Bessel Functions.* Cambridge University Press.

DEPARTMENT OF STATISTICAL SCIENCE
DUKE UNIVERSITY
DURHAM, NORTH CAROLINA 27708-0251
USA
E-MAIL: ml371@stat.duke.edu

DEPARTMENT OF STATISTICS
NORTH CAROLINA STATE UNIVERSITY
RALEIGH, NORTH CAROLINA 27695-8203
USA
E-MAIL: sghosal@stat.ncsu.edu